Polymer Chemistry

REVIEW

View Article Online
View Journal | View Issue

Cite this: *Polym. Chem.*, 2019, **10**, 2906

Recent advances in colloidal nanocomposite design *via* heterogeneous polymerization techniques

Stuart C. Thickett * and Guo Hui Teo

Received 21st January 2019,
Accepted 14th March 2019

DOI: 10.1039/c9py00097f

rsc.li/polymers

The design and synthesis of composite nanoparticles consisting of a polymeric phase and an inorganic/organic phase has enjoyed a period of extensive development in recent times due to numerous advances in heterogeneous polymerization. In this review, we look at several key advances that have shaped this field in the past decade. Specifically, advances in encapsulation technologies *via* emulsion and miniemulsion polymerization are considered, in addition to the advent of polymerization-induced self-assembly (PISA) that has afforded morphological control of such composites. The use of nanomaterials as particle (Pickering-type) stabilizers is also discussed as a method of generating composite nanoparticles in one step. Specific applications of these nanocomposites in terms of materials properties are also highlighted.

School of Natural Sciences (Chemistry), University of Tasmania, Hobart, TAS 7005, Australia. E-mail: stuart.thickett@utas.edu.au

Stuart C. Thickett

Stuart Thickett is a Senior Lecturer in Chemistry at the University of Tasmania. He received his PhD from the University of Sydney in 2008 under the supervision of Professor Robert Gilbert in the area of emulsion polymerization kinetics and mechanism. He has held a post-doctoral position at the University of Toronto, and the University of Sydney, working in the areas of polymer nanoparticle and polymer thin film design. In 2012 he joined the Centre for Advanced Macromolecular Design (CAMD) at UNSW as a Vice-Chancellor's Research Fellow, and was appointed Lecturer at the University of Tasmania in 2015. Stuart's research interests primarily focus on the physical chemistry of soft matter, namely polymer nanoparticles, colloids and interfaces, where he utilizes advanced polymerization techniques for the design of new materials. Stuart has published 49 journal articles in his career to date and presented his work at over 70 national and international conferences.

Introduction

The history of polymer composites and their applications spans several decades, driven by the desire to create materials that have a specific function or property. Examples include the enhancement of mechanical or thermal properties relative to the neat polymer,[1] sensing applications,[2] catalytic activity,[3] response to an applied magnetic field,[4] or superior performance as a surface coating.[5,6] Numerous methods exist to prepare polymer composite materials, such as solution blending or melt processing, however these methods are relatively irreproducible and are often characterized by aggregation or phase separation of the organic/inorganic phase.[7]

An alternative method towards the preparation of composite materials is to prepare them on the nanoscale as a hybrid colloid or "latex". Colloidal nanocomposites, as they will be referred to in this review, represent a class of nanomaterials that have been the subject of extensive research interest in both academia and industry.[8,9] Specifically, they utilize one of the major heterogeneous polymerization methods (such as miniemulsion,[10–12] emulsion[13,14] and dispersion polymerization[15,16]), where an organic monomer is polymerized, most typically in water or an alcohol in the presence of a stabilizer, yielding polymer particles typically below 1000 nm in diameter. The production of composite particles is achieved typically through two main approaches: (i) the inclusion of preformed organic or inorganic nanoparticles into the polymerization, or (ii) the use of a precursor or auxiliary co-monomer to promote composite formation as a second step. The range of materials combined with the polymeric phase is highly diverse, including metal (or semi-metal) oxide

nanoparticles,[17–24] colloidal semiconductors ("quantum dots",[25–27] as well as two-dimensional platelet materials such as clays,[28–32] graphene,[33–37] graphene oxide[38–42] and reduced graphene oxide.[43,44] Both approaches towards colloidal nanocomposite synthesis have advantages and drawbacks (as an example, the use of pre-formed nanoparticles requires control of surface chemistry to ensure effective encapsulation), and are often more suited to a particular type of heterogeneous polymerization mechanism. Significant advances in controlling polymerization, such as the advent of reversible deactivation radical polymerization (RDRP) in dispersed systems,[45–48] has recently enabled morphological control in nanocomposite design not previously possible.

In this review, we consider recent advances in the preparation of nanocomposite materials, specifically by heterogeneous polymerization methods. We largely restrict discussion to advances made in the past decade (2010 onwards), however where relevant, key works prior to this are included for completeness. Arguably one of the most significant advances in polymer nanoparticle synthesis in recent times, polymerization-induced self-assembly (PISA), is also reviewed in the context of nanocomposite synthesis. The review is structured on the basis of polymerization mechanism, and naturally there are areas where overlap occurs (*e.g.* emulsion polymerization and polymerization-induced self-assembly). We focus on achievements with respect to controlling the resulting particle morphology of the colloidal nanocomposite, by addressing the following questions: (i) How can efficient and effective nanoparticle encapsulation be achieved in heterogeneous polymerization? and (ii) What methods enable the formation of "armoured" (*i.e.* polymeric core/nanoparticle shell) structures? Examples of the use of these nanocomposites in various materials science applications are also highlighted.

Miniemulsion polymerization

Miniemulsion polymerization has been arguably the method of choice in the preparation of colloidal nanocomposites, based on the extensive array of examples in the literature.[10,49–54] One of the major advantages of miniemulsion polymerization is the particle formation mechanism, which relies on the direct polymerization of a fine dispersion of monomer droplets, typically produced by ultrasound or the application of high energy emulsification (Fig. 1). This idealized mechanism results in a 1-to-1 "copy" of the monomer droplet distribution being converted into the final distribution of polymer particles, however in reality significant deviations from this can occur due to phenomena such as Ostwald ripening.[55] Miniemulsion polymerization is also a particularly appealing method for generating hollow particles or polymer capsules for specific applications such as encapsulation and release.[10] For the production of composite nanoparticles, the effective dispersion of another material (*e.g.* an inorganic nanoparticle such as silica, titania, iron oxide, *etc.*) in the monomer phase prior to emulsification can result in "loaded" droplets that can achieve the desired morphology.

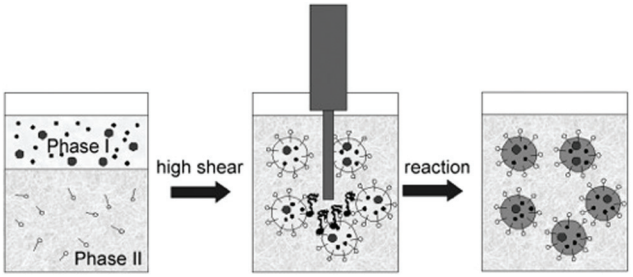

Fig. 1 Schematic of the miniemulsion polymerization process. Reproduced with permission from ref. 10. Copyright 2009, John Wiley and Sons.

In this section we discuss recent advances in miniemulsion polymerization for composite design based around two main thematic areas – the use of pre-formed composite materials (*i.e.* nanoparticles), and the use of inorganic precursors and/or auxillary monomers that facilitate the formation of a composite material post-polymerization. Emerging research areas and applications are also highlighted.

Morphological control with pre-formed particles – armoured or encapsulated?

Morphological control of composite particles is particularly important with a view towards the final application of the material. For example, the full encapsulation of an inorganic nanoparticle (*e.g.* a pigment) within the polymer phase is desirable for film-forming systems, as this ensures an homogeneous distribution of the material throughout the resultant polymer matrix.[56] Alternatively, 'armoured' particles (such as those prepared by Pickering stabilization) may be the desired morphology for materials with functional surfaces[3] or film-forming systems with targeted mechanical properties.[31]

When considering the batch miniemulsion polymerization of a vinyl monomer with pre-formed inorganic nanomaterial dispersed within, the final particle morphology at the conclusion of polymerization is influenced by both reaction kinetics and the thermodynamics of the system. Asua developed a morphological map for predicting the equilibrium particle morphology (Fig. 2),[57] which is related to the various values of the interfacial tension between the polymeric (P), inorganic (I) and aqueous (W) phases respectively. Depending on the relative values of the interfacial tension between the three phases, the resultant morphology can be encapsulated, "armoured", hemispherical/Janus, or no encapsulation (with respect to the inorganic phase relative within the polymer phase). Reported values of interfacial tensions for various materials are scarce and so as a result one of the most powerful aspects of this morphological map is to understand key trends in influencing morphology by changing, for example, initiator type, monomer type, surfactant (if employed), and the role of surface modification of the inorganic nanomaterial. The utility of this morphology map was recently demonstrated by Aguirre

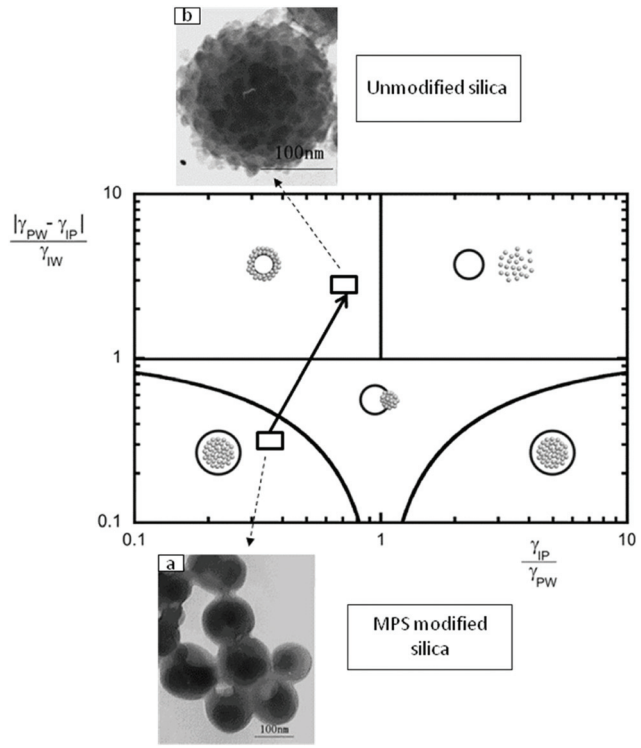

Fig. 2 Morphological map describing the thermodynamically favoured morphologies for composite particles based on the interfacial tensions between the polymeric (P), inorganic nanoparticle (I) and water (W) phase. Examples of modified (a) and unmodified (b) silica nanoparticles with respect to polystyrene–silica composites are shown. Reproduced with permission from ref. 57. Copyright 2014, John Wiley and Sons.

et al.,[56] where the morphology of acrylic/ceria nanoparticles changed from encapsulated to hemispherical upon the addition of a polymeric hydrophobe.

Surface modification of the inorganic material is particularly relevant as it represents a convenient method to improve the dispersibility of the material in the monomer phase, *e.g.* the surface modification of bare silica nanoparticles with a relevant hydrophobic or functional silane. Surface modification reduces the I–P interfacial tension while increasing the I–W interfacial tension, resulting in an associated shift from an armoured morphology (*i.e.* silica nanoparticles at the interface of the polymer particle) to an encapsulated morphology (see insets of Fig. 2). The role and relevance of surface modification with respect to nanocomposite design is discussed in the context of specific examples below.

Silica. Arguably the most studied class of nanoparticles in the context of hybrid polymer–inorganic material synthesis, either *via* miniemulsion polymerization or other means, is silica (SiO_2). Silica nanoparticles are conveniently synthesized by simple methods (such as Stober synthesis[58]) on a large scale and are commercially available in a wide range of differing particle sizes. Importantly, the surface of silica nanoparticles can be readily functionalized or modified. The application of silica nanoparticles is diverse, spanning areas such as controlled release and energy storage.[59,60]

The ready surface modification of silica nanoparticles (through functionalization of surface silanol groups) enables them to be rendered hydrophobic (and hence dispersible in the droplet phase) and/or polymerizable for effective dispersion in the polymeric matrix *via* surface cross-linking. The diversity of approaches here is numerous, with one of the most popular routes being the use of polymerizable silanes such as (3-trimethoxysilyl)propyl methacrylate (MPS).[61–65] Bourgeat-Lami *et al.*[66] has shown the importance of MPS modification in effective dispersion of silica into the monomer phase (in their case, a MMA/BA mixture), with raw (unmodified) silica nanoparticles undergoing significant agglomeration when dispersed in MMA; MPS-functionalized silica was able to be effectively dispersed with narrow particle size distribution. The choice of monomer is also relevant when dispersing MPS-modified silica (*e.g.* agglomeration was shown to occur upon dispersion in BA, but not in a MMA/BA mixture), in addition to solids content. Through the use of cryo-TEM, the distribution of MPS-silica nanoparticles within monomer droplets was studied, revealing a strongly heterogeneous distribution that was replicated in the resultant polymer latex. Further relevant to the morphology of the resulting composite, the MPS-silica particles were shown to be localized at the monomer/water interface (Fig. 3), suggesting a particle stabilizer (Pickering) type effect.

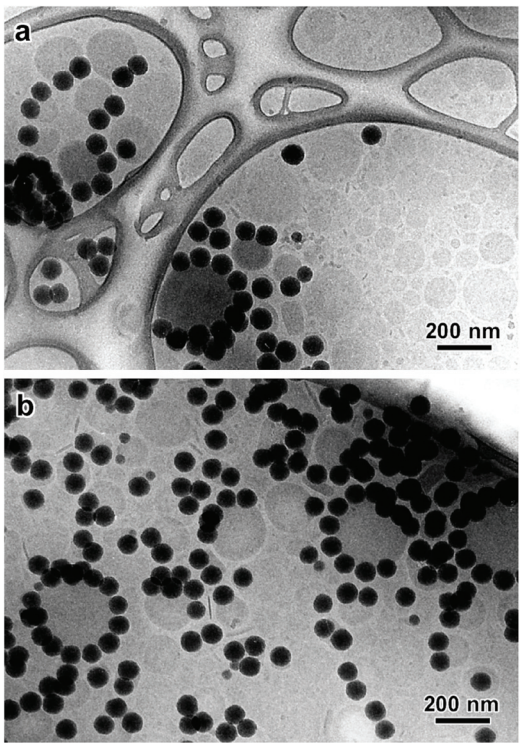

Fig. 3 Cryo-TEM images of miniemulsion droplets consisting of MPS-modified silica nanoparticles (10% w/w) dispersed into a 50/50 w/w mixture of MMA/BA, prior to ultrasonication with water. Reprinted with permission from E. Bourgeat-Lami, G. A. Farzi, L. David, J. L. Putaux and T. F. L. McKenna, *Langmuir*, 2012, **28**, 6021–6031. Copyright 2012 American Chemical Society.

Both Mirmohseni *et al.*[67] and Sanei *et al.*[68] used alternative surface modification methods to incorporate silica nanoparticles into MMA/BA/MAA copolymer latexes prepared by miniemulsion polymerization. Mirmohseni used methylene diphenyl diisocyanate (MDI) to modify silica particles dispersed in toluene, followed by addition of 2-hydroxyethyl methacrylate (HEMA) to give methacrylic functionalities at the silica particle surface. Sanei directly reacted surface silanol groups with glycidyl methacrylate under acidic conditions, reporting 92% encapsulation efficiency of the modified silica following miniemulsion polymerization (at an initial loading of 5% w/w modified silica). These formulations were film forming and when cast as a film, greatly improved scratch resistance was reported upon inclusion of the modified silica phase compared to the neat polymer.

Whereas hydrophobic modification enables silica nanoparticles to be encapsulated *via* miniemulsion polymerization, particles with an armoured morphology can potentially be prepared using hydrophilic silica as particle stabilizer. Using a commercially available silica sol with glycerol surface, Zhang *et al.* recently prepared composite nanoparticles consisting of a polystyrene or poly(styrene-*co*-butyl acrylate) core and a shell of silica nanoparticles.[69] A raspberry-type morphology was observed with silica nanoparticles adsorbing at the particle interface, and it was shown that the choice of surfactant was critical to promote the desired morphology. When a cationic surfactant (CTAB) was used to prepare the miniemulsions, silica adsorption was observed, but not when the anionic surfactant sodium dodecyl sulfate (SDS) was employed. No silica adsorption at the polymer particle interface was observed when the glycerol functionality was absent (Fig. 4), similar to previous work by Schmid *et al.* in composite preparation *via* emulsion polymerization.[70–72]

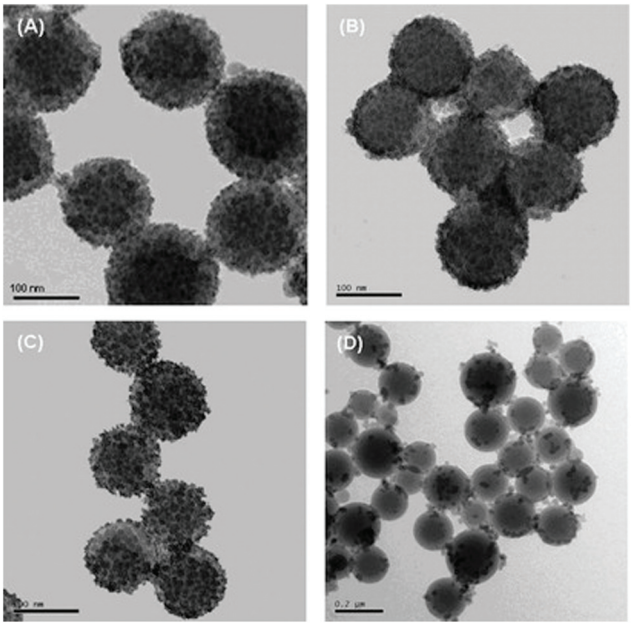

Fig. 4 Polystyrene particles with a shell of glycerol-functionalized silica nanoparticles prepared by miniemulsion polymerization. Figures (A)–(C) represent particles prepared with increasing amounts of the cationic surfactant CTAB. Figure (D) is the equivalent synthesis in the presence of silica nanoparticles without glycerol functionality at the surface. Reproduced with permission from ref. 69. Copyright 2013, Taylor and Francis.

Iron oxide. The preparation of composite polymer nanoparticles with incorporate iron oxide (specifically magnetite) has been extensively studied in miniemulsion polymerization, due the ability to readily prepare particles that exhibit a response to an applied magnetic field. Applications of such response include magnetic affinity separation, as well as applications in magnetic resonance imaging (MRI) and hyperthermia.

The most common method of encapsulation of magnetite nanoparticles is to render the surface of the nanoparticles hydrophobic (*via* attachment of an appropriate surface modifiers) in order to facilitate their dispersion in the monomer phase. For this purpose, oleic acid (OA) is one of the most common surface modifiers.[73–81] In order to increase the loading of magnetite, Landfester's group has pioneered processes based on multiple miniemulsions.[82–86] As an example, OA-coated magnetite was first dispersed in octane and then miniemulsified into droplets stabilized by SDS. The octane was allowed to evaporate, followed by mixing this dispersion with another miniemulsion of St droplets and subsequent polymerization. This "ad-miniemulsion" process has also been used to facilitate clay platelet encapsulation[87] as well as carbon black[86] and pigment particles.[85]

The major drawback of the above-mentioned approach is the use of multiple steps to prepare the composite particles. Recently, Ramos and Forcada[88] have demonstrated a single-step method of magnetite encapsulation into polystyrene nanoparticles prepared by miniemulsion polymerization. In their work, OA-coated iron oxide nanoparticles were directly dispersed into a styrene/HD mixture at a weight fraction of 40% w/w. This oil phase was miniemulsified with an aqueous dispersion of initiator (KPS), and in some instances a water-soluble crosslinker/stabilizer ([2-(methacryloyloxy)ethyl] phosphate, BMEP) and stabilizers (SDS or dextran) in varying quantities. It was shown that a mixed stabilizer system (OA plus 2% w/w BMEP) was advantageous towards ensuring a high amount of "loaded" polymer particles (>90% of particles containing iron oxide), with dextran ensuring small final particle size and narrow particle size distribution. In a similar vein, van Berkel *et al.* also demonstrated the importance of the "right stabilizer" for nanoparticle encapsulation in miniemulsion polymerization.[11,89] They used short polystyrene oligomers to functionalize metal nanoparticles for excellent dispersion into emulsified divinylbenzene droplets prior to polymerization, with the loading of the metal nanoparticles as high as 33% w/w relative to monomer.

Clay platelets. Clay platelets have been extensively utilized in the design of polymer composites, primarily due to the excellent gas barrier properties and improved hardness/scratch resistance conferred on the resulting material.[90–92] When fully

exfoliated, clays are essentially 2D nanomaterials with lateral dimensions ranging from ~25 nm through to several hundred nanometres. As clay platelets can be readily dispersed in water,[93] surface modification is required for encapsulation in miniemulsion systems. They can also act as Pickering stabilizers to generate armoured particles by the miniemulsion polymerization of various monomers as shown by Bon *et al.*,[28,94] as well as inverse miniemulsion polymerization by the group of van Herk[95] in addition to emulsion polymerization[5,96] (discussed in the following section).

An example of the role that clay type and method of modification has with respect to particle morphology was demonstrated by Zengeni *et al.*[32] Using an ad-miniemulsion approach, small LAPONITE® clay platelets (size 25–40 nm) and larger montmorillonite (MMT) platelets (ranging from 50–500 nm) were first modified with the non-reactive CTAB or the polymerizable surfactant vinylbenzyldodecyltrimethylammonium chloride (VBDAC), followed by mixing with a styrene (St) miniemulsion and subsequent polymerization. The effect on morphology was significant – for the smaller LAPONITE® clay platelets, modification with VBDAC resulted in encapsulation and dispersion within the PSt particle; use of CTAB as modifier resulted in an armoured morphology. The encapsulated PS/LAPONITE® system gave a 13 °C increase in T_g relative to the neat polymer at a LAPONITE® loading of 50% w/w, whereas the change to T_g was negligible in the case of armoured particles. The larger MMT platelets gave armoured or "sandwich"-type morphologies in both cases.

Clay platelets have seen application as Pickering stabilizers in film-forming systems for specific applications prepared by both miniemulsion and emulsion polymerization. Chakrabarty *et al.* utilized LAPONITE® RDS clay as a Pickering stabilizer for the RAFT-mediated miniemulsion polymerization of 2,2,3,3,3-pentafluoropropyl acrylate, MMA and BA in order to prepare low surface energy surface coatings.[30] In order to make LAPONITE® sufficiently hydrophobic to act as a Pickering stabilizer, a cationic RAFT agent *S*-1-dodecyl-*S*′-(methylbenzyl triethylammonium bromide) trithiocarbonate was first mixed with an aqueous dispersion of LAPONITE® in order to promote electrostatic attraction between the two. The role of the charged RAFT agent was significant on polymerization kinetics, with a ten-fold increase in reaction rate compared to the corresponding neutral RAFT agent. LAPONITE® loadings of up to 40% w/w were possible, with morphological analysis by TEM clearly showing armoured spherical nanoparticles approximately 200 nm in diameter. When cast as films, a high static water contact angle (102.4°) was observed. Bonnefond *et al.*[6] also demonstrated the preparation of composite films with greatly reduced water vapour transmission when montmorillonite platelets were used as stabilizers for the preparation of styrene-*co*-butyl acrylate latexes.

Graphene oxide. The past decade has seen significant activity in the design of polymer–graphene composite materials through the use of graphene oxide (GO) as a precursor material, followed by reduction (chemical or otherwise) back to a graphene-like material.[33,35,36,97–99] GO, the oxidation and exfoliation product of graphite, is readily produced on a large scale, and significantly is amphiphilic in nature[100,101] with the ability to act as a Pickering stabilizer.[102,103] The amphiphilic nature of GO is dependent on the lateral dimensions of the GO sheets, level of oxidation, and pH of the dispersed phase,[104,105] which enables convenient tuning of emulsion stability.

GO sheets of varying size have been used as Pickering-type stabilizers for the miniemulsion polymerization of various monomers. Song *et al.*[106] performed the miniemulsion polymerization of styrene (St) in the presence of GO sheets of a variety of sizes, whereby armoured particles were formed in the presence of small (~300 nm) sheets, and alternatively PSt particles decorating the surface of large GO sheets (of the order of several microns). The miniemulsion polymerization of MMA has also been reported[107] where stable miniemulsions were only formed above 4% w/w of GO sheets relative to the monomer. The resulting composite had a greater Young's modulus than PMMA, at the expense of increased brittleness.

Demonstrating the influence of surface modification with regards to composite particle morphology, Etmimi *et al.* used a reactive surfactant (2-acrylamido-2-methyl-1-propanesulfonic acid, AMPS)[38] or RAFT agent (dodecyl isobutyric acid trithiocarbonate)[39] to modify GO sheets prior to the miniemulsion polymerization of styrene/*n*-butyl acrylate and styrene respectively. 80% w/w of AMPS (relative to GO) was used, and the miniemulsion was stabilized by SDBS. The modified sheets were observed to be "stacked" within the particle interior; RAFT modified GO sheets also provided moderate control of the resulting MWD of the polymer ($Đ$ values ranging from 1.26–1.62). As composite materials, an enhancement in both thermal stability as well as storage and loss moduli was observed relative to the neat polymer when the GO loading was >3% w/w with respect to the polymer.

The group of Pentzer has investigated the preparation of modified GO nanosheets *via* numerous functionalization methods, often with a view towards the synthesis of armoured particles with reactive surfaces.[108–112] Exploiting the reactivity of GO sheets towards nitriles[109,112] through reaction with surface hydroxyl groups, both small molecule and polymeric functionalization with accompanying partial reduction of GO has been reported. The reaction of GO with acrylonitrile in aqueous systems results in the formation of acrylate groups on the surface of the material;[108] this acrylate-functionalized GO was then further modified with thiol-terminated polymers *via* base-catalysed thiol–ene "click" chemistry. A particularly elegant example of monofacial and bifacial functionalization of GO was demonstrated with these materials by using acrylate-functional GO as a Pickering stabilizer for the preparation of a toluene-in-water miniemulsion, followed by different thiol–ene reactions in the two phases (*e.g.* reaction with thiol-terminated polystyrene in the toluene phase, and thiol-terminated poly(acrylic acid) in the aqueous phase. These Janus GO sheets were shown to greatly reduce the interfacial tension compared to monofunctional or nonfunctional GO. The use of allyl isocyanate to functionalize GO has also been reported,

with the resultant nanosheets used to stabilize polythioether nanoparticles prepared by photoinitiated thiol–yne miniemulsion polymerization.[111] GO functionalization with alkylamines of differing chain length has enabled the Pickering stabilization of non-aqueous miniemulsion systems,[110] such as dodecane-in-DMF (and *vice versa*). These all-oil-based systems open the pathway to heterogeneous polymerization of water-sensitive reagents such as methacrylates with pendant isocyanate groups, or interfacial step-growth polymerization.

Work by the group of Zetterlund and the authors of this manuscript has exploited the inherent surface activity of GO nanosheets for the miniemulsion polymerization of various vinyl monomers in the absence of additional surfactant (Fig. 5).[40,113–118] Using very small GO sheets (~30 nm in diameter, derived from graphite nanofibres), the successful miniemulsion homopolymerization of styrene and various methacrylates has been reported, in addition to film-forming systems (*e.g.* the copolymerization of styrene with BA[118]). In these systems, "armoured" particles (consisting of a shell of GO sheets) were observed by TEM and SEM analysis. Using cross-linkers such as divinyl benzene (DVB) and ethylene glycol dimethacrylate (EGDMA) and a high loading of non-solvent (hexadecane, typically 50 w/w%),[40,115] hollow capsules stabilized with GO sheets were also prepared by this approach. These capsules were shown to have relatively high surface area (~250 m^2 g^{-1}) and an accessible internal void volume *via* surface mesoporosity, raising the possibility of applications in catalysis and encapsulation. The electrically insulating nature of GO has led us in recent times to explore the preparation of composite films prepared by the above-mentioned miniemulsion approach, followed by thermal reduction to potentially yield electrically conducting films.

Titanium dioxide. Titania (TiO_2) nanoparticles find application in numerous polymer composites, particularly films and surface coatings, due to its high refractive index and effective use as a pigment. A semi-conductor, titania also is used heavily in photocatalysis, particularly in aqueous systems where environmental pollutants undergo photodegradation.[119]

Without surface modification, the effective dispersion of titania into the monomer phase for miniemulsion polymerization is not possible. The group of El-Aasser[120–122] first demonstrated the effective surface modification of P25 (a mixture of ~70% anatase with minor rutile and amorphous components, however the composition can vary) with the commercial stabilizer OLOA370 (polybutylene succinimide diethyl triamine), which was then used in the miniemulsion polymerization of styrene. At a loading of 5% w/w (relative to the monomer phase), the encapsulation of modified titania was as high as 92%; the polymer particle size was typically much larger in the presence of modified titania compared to the neat particles. More recently, Li *et al.*[123] has used sodium stearate to render the surface of 10 nm anatase particles hydrophobic, for dispersion into a MMA–BA–AA mixture for the preparation of hybrid latexes by miniemulsion. The authors claimed a multilayer structure with a hydrophobized titania core embedded within a (meth)acrylic polymer phase, with un-modified (hydrophilic) titania present at the particle surface, formed potentially *via* physi- or chemisorption from the continuous phase.

Titania nanoparticles have also been used as Pickering stabilizers in miniemulsion polymerization. Chen *et al.*[24] used unmodified titania as a Pickering stabilizer to prepare hollow capsules by miniemulsion polymerization, with the capsules ranging from 10 to 50 μm in diameter. González *et al.*[3] used nanoparticles that were surface modified with acetylacetone and *para*-benzenesulfonic acid as Pickering stabilizers, as these nanoparticles were shown to have close to ideal wettability characteristics with respect to the oil/water interface. At a loading of 5–20% w/w with respect to the monomer phase, a mixture of MMA, BA and octadecyl acrylate (the octadecyl acrylate also acting as a hydrophobe) was polymerized to yield armoured particles that decreased in average size (from over

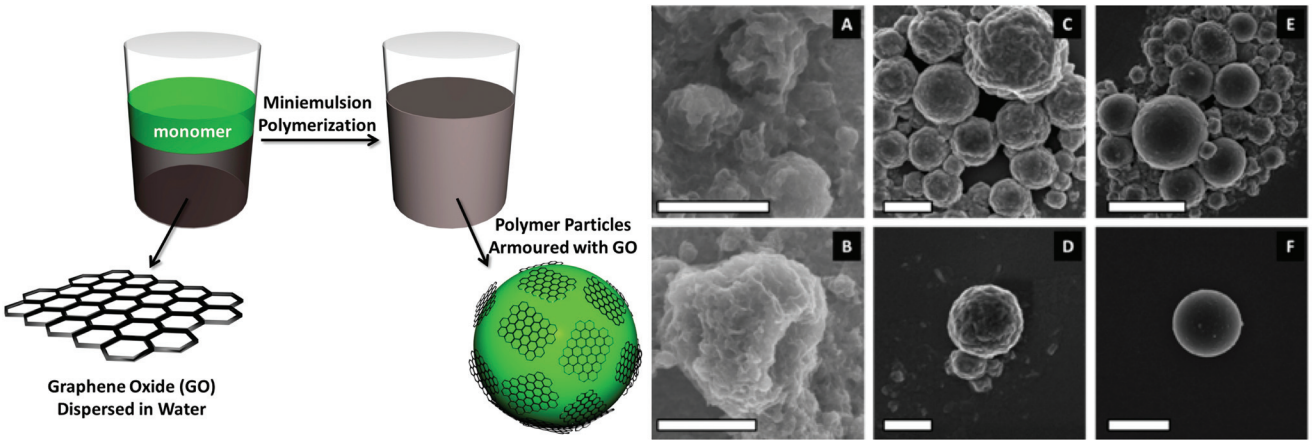

Fig. 5 Miniemulsion polymerization of styrene stabilized solely by GO nanosheets. Left: schematic of the process. Right: SEM images of the resulting particles at 19% (A, B), 47% (C, D) and 90% (E, F) conversion of monomer. Scale bars = 500 nm for A–D, 2000 nm for E–F. GO loading was 7.5% w/w relative to the monomer. Adapted and reproduced with permission from ref. 113. Copyright 2013, John Wiley and Sons.

1 micron to 370 nm) upon increasing the loading of titania. The composite particles formed films at room temperature with increased opacity at higher titania loadings. The films were shown to exhibit a self-cleaning property, with the degradation of Rhodamine B demonstrated upon exposure to UV light. The group of Du has also shown the importance of surface modification of titania with respect to effective Pickering miniemulsion formation.[124–126]

Emerging areas. Several emerging topics have become more prevalent in recent years with respect to colloidal nanocomposites by miniemulsion polymerization. Inspired by the use of silver nanoparticles in applications such as wound healing and antimicrobial coatings, Mamaghani *et al.* recently demonstrated the incorporation of unmodified colloidal nanosilver into poly(methyl methacrylate-*co*-butyl acrylate-*co*-acrylic acid) latexes prepared by miniemulsion polymerization.[127] This was achieved by dispersing silver nanoparticles in an aqueous solution of various emulsifiers and stabilizers (poly (vinylpyrrolidone), Kenon40 and cetyl alcohol) prior to ultrasonication in the presence of the monomer mixture. The resulting composite particles were shown to possess antibacterial activity towards Gram-positive and Gram-negative bacteria, with a greater region of inhibition than was achieved by simple mixing of the neat latex and silver nanoparticles.

There has been a significant drive recently towards the use of renewable resources (*i.e.* not derived from petroleum feedstocks) in polymer chemistry as well as in the preparation of composite materials. This is reflected in recent work utilizing materials derived from biomass in the preparation of composites *via* miniemulsion polymerization.[1,128] Jairam *et al.* used lignin derived from biorefinery waste to prepare clay (saponite)–lignin hybrids that were incorporated into a styrene–butyl acrylate miniemulsion system, stabilized by Triton TX-405.[128] The resultant latex was used to create composite films that exhibited >40% reduction in oxygen permeability and a 14-fold increase in tensile strength compared to the neat polymer. The use of cellulose-derived materials such as cellulose nanocrystals (CNCs) or nanofibers (CNFs) have attracted significant research interest; in particular they have relevance as bio-based Pickering stabilizers.[129–132] Errezma *et al.* recently incorporated cellulose nanofibers into particles of poly(butyl methacrylate) prepared by miniemulsion polymerization,[1] using a preformed cationic copolymer to drive electrostatic incorporation of the negatively charged CNFs to the particle surface. At a loading of 8% w/w CNFs relative to polymer, a 200-fold increase in stiffness and 13-fold increase in tensile strength was observed. The group of Cranston has also demonstrated the successful miniemulsion polymerization of MMA using a mixture of CNCs and oppositely charged ionic surfactant as a mixed surfactant system,[129] in addition to a mixture of CNCs with methylcellulose.[132]

Composite particles *via* inorganic precursors

An alternative to pre-formed inorganic nanoparticles in miniemulsion polymerization is the use of precursors or auxillary monomers that enable the *in situ* formation of the composite material within the resulting polymer nanoparticle. By this method, the issue of effective encapsulation is removed, although phase separation at the nanoscale can still result in the formation of different final particle morphologies. The most common demonstration of this approach is the use of commercially available alkoxysilanes such as tetraethylorthosilicate (TEOS) that will undergo hydrolysis and condensation to form silica, typically *via* base catalysis. Polymerizable silanes such as MPS (often used for surface modification as discussed in the preceding section) are also attractive given that they readily copolymerize into styrenic, acrylic or methacrylic formulations, enabling subsequent reaction of the pendant trialkoxysilane.[133–136]

The use of MPS as a functional comonomer in miniemulsion polymerization has been demonstrated by several groups.[137–141] Droplet nucleation is advantageous when working with monomers such as MPS, as the premature hydrolysis and condensation of alkoxysilyl groups that can occur is suppressed.[139,142] Due to differences in interfacial tension, the particle interface in such systems is enriched with reactive alkoxysilyl groups that can be functionalized or coated with a silica shell *via* the controlled hydrolysis and condensation of TEOS at the particle surface. An analogous approach has also been used in emulsion polymerization systems,[143,144] where subsequent removal of the polymeric core enables the formation of hollow capsules.

Recent examples in the use of silica precursors in miniemulsion polymerization have involved the formation of non-spherical particle morphologies, producing "lobed" particles or raspberry-like structures. Zhang *et al.*[69] prepared composite nanoparticles *via* the miniemulsion polymerization of MMA and MPS (mass ratio of MMA : MPS = 10), with TEOS also present in the dispersed phase (MMA : TEOS = 2) prior to emulsification with an homogenizer. Following a brief interval of polymerization at 75 °C for 30 min, ammonia was added to the continuous phase to promote the hydrolysis and condensation of TEOS domains to form silica. The success of this approach is driven by the phase separation of TEOS domains to the droplet interface upon polymerization. A similar approach was used by Yang *et al.*[145] where the miniemulsion polymerization of styrene, divinylbenzene (DVB), MPS and TEOS (in a mass ratio of 7 : 1 : 3 : 30) was performed using a redox initiation pair, where one component (cumene hydroperoxide) was dissolved in the oil phase and the other (tetraethylenepentamine) in the aqueous phase, in order to ensure radical generation at the droplet interface. Following polymerization, the addition of base enabled silica domains to be formed at the particle interface, achieving raspberry-like particles approximately 200 nm in diameter. Zhang *et al.*[146] also reported the synthesis of raspberry-like particles by first hydrolysing MPS in a pH 4 aqueous medium, followed by mixing with styrene and subsequent ultrasonication. Prior to polymerization, a basic dispersion of 50 nm diameter silica nanoparticles was added, which underwent condensation with the silanol groups at the droplet interface, generating the targeted raspberry morphology.

The use of silica precursors can also be used to prepare targeted Janus-type colloidal nanocomposites, typically driven by phase separation within the nanoparticle during hydrolysis and condensation of the alkoxysilane. Zhang *et al.* performed the miniemulsion polymerization of St, MPS and TEOS stabilized by SDS,[147] whereby after a short interval of polymerization under neutral conditions, the pH of the continuous was adjusted to 9.0 to promote TEOS hydrolysis and condensation. As the TEOS is immiscible with the formed PSt domains, the increase in pH resulted in the TEOS "lobe" being converted into a silica nanodomain within the particle structure, as confirmed by electron microscopy. A similar approach was used by Han *et al.*[148] to prepare PSt/silica/ZnO Janus nanocomposites, where hydrophobic ZnO nanoparticles were first dispersed into a St/TEOS mixture followed by miniemulsification, polymerization and silica formation.

The use of inorganic precursors is not solely confined to the *in situ* generation of silica. Other examples include the use of titania precursors (*e.g.* tetra *n*-butyl titanate, TBT). Wu *et al.*[149] reported a one-step method for the formation of polystyrene/titania nanoparticles *via* miniemulsion polymerization through the use of TBT loaded into the pre-formed monomer droplets. In this work, acetylacetone was added to the styrene/hexadecane phase to act as a chelating agent for the added TBT. Nanophase separation during polymerization was observed by TEM, with 60–80% of the total titania content found by XPS to be at the polymer particle interface.

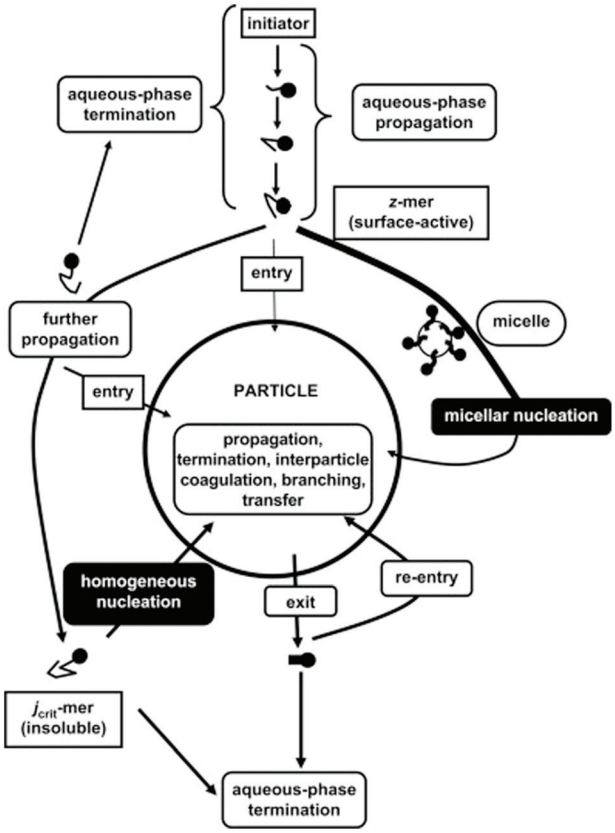

Fig. 6 Mechanistic overview of *ab initio* emulsion polymerization in the presence of surfactant. Reproduced from S. C. Thickett and R. G. Gilbert, *Polymer*, 2007, **48**, 6965–6991, available under a CC BY-NC-ND 3.0 Creative Commons licence.

Emulsion polymerization

Emulsion polymerization is unquestionably the most common method for the preparation of aqueous dispersions of polymeric nanoparticles on an industrial scale. Mechanistically distinct from miniemulsion polymerization, emulsion polymerization does not require high shear/ultrasound or the addition of ultrahydrophobes, and can be routinely performed in the absence of added surfactant. Droplet nucleation in emulsion polymerization is typically negligible, with the resulting particle phase formed either *via* micellar or homogeneous nucleation (Fig. 6).[150–155] While experimentally simple to perform, these particle formation mechanisms have made the formation of encapsulated composite materials particularly challenging until recent times. In this section, we review key advances in emulsion polymerization composite synthesis, in particular where reversible deactivation radical polymerization (RDRP) techniques are used to facilitate effective encapsulation. The use of nanoparticles as particle-based surfactants (*i.e.* Pickering emulsion polymerization) is also an active research area for the design of polymer composites in the absence of surfactant, described below.

Pickering emulsion polymerization

The use of particles as colloidal stabilizers has been known for over a century.[156,157] The resulting emulsion, often referred to as a "Pickering emulsion," thus represents a convenient route towards colloidal nanocomposite synthesis. Advantageously, Pickering-type systems do not require the addition of low molecular weight surfactants that can have potentially deleterious effects in the final product (*e.g.* a composite film). Particle stabilizers have seen extensive use in both miniemulsion (as detailed in the preceding section) and emulsion polymerization.[158]

As miniemulsion polymerization relies on droplet nucleation, the mechanism of particle formation with Pickering stabilizers occurs *via* the adsorption of nanoparticles at the droplet/water interface. The story is not so clear in the case of emulsion polymerization. Compared to the kinetics and mechanism of "traditional" (*e.g.* surfactant-stabilized or surfactant-free) emulsion polymerization that are arguably well understood,[150,151,159–161] there remain unanswered questions regarding particle formation and growth kinetics in Pickering emulsion polymerization systems. In particular, interfacial processes (such as radical entry[162] and exit into and out of a polymer particle) are likely to be influenced by the presence of Pickering stabilizers at the particle interface; furthermore, the particle nucleation process[160] in such systems is dependent on numerous factors discussed below.

Numerous groups have shown that successful particle formation in Pickering emulsion polymerization, achieving an armoured morphology with high coverage of stabilizer par-

ticles, is reliant on several factors. Arguably the most important parameter is the chemical nature of the monomer/polymer itself, which influences successful particle adsorption at the interface. Siilica nanoparticles have been shown to absorb to the surface of MMA-based latexes, but not more hydrophobic styrene or butyl methacrylate latexes.[163] Percy *et al.*[164,165] showed that 4-vinylpyridine (4VP) as co-monomer enabled the surfactant-free emulsion polymerization of various monomers in the presence of silica nanoparticles; the acid–base interaction between 4VP and silica promoted particle adsorption and composite formation. A similar effect was observed in the emulsion polymerization of MMA with 1-vinylimidazole (10% w/w relative to MMA) in the presence of silica nanoparticles.[166] PEG-based auxiliary co-monomers are also often used to promote silica nanoparticle adsorption[13] and clay platelet adsorption[5,167] in emulsion polymerization, exploiting the strong interaction between PEG chains and these nanomaterials. Hydrophilic monomers such as methacrylic acid have also been used in small amounts to promote clay adsorption to the surface of styrene–BA latexes.[168] Particle adsorption is often dependent on the pH and/or ionic strength of the continuous phase, as this influences the zeta potential as well as any barrier towards adsorption of the nanoparticle at the polymer interface.

To address these mechanistic questions, detailed kinetic experiments regarding Pickering emulsion polymerization stabilized by LAPONITE® clay platelets[169] and silica nanoparticles[170] have been reported recently. Brunier *et al.*[169] studied the *ab initio* and seeded emulsion polymerization experiments using LAPONITE® RDS clay as stabilizer. In seeded experiments, the polymerization rate (and hence average number of radicals per particle) was shown to be independent of the initial clay concentration. *Ab initio* experiments showed that an increase in the initial clay concentration resulted in increased polymerization rate and a greater number of (smaller) nucleated polymer particles, suggesting an important role of the clay in stabilizing newly nucleated particles. Modelling of the resultant particle size distributions enabled the radical capture efficiency to be determined; importantly, no hindrance to radical capture due to the presence of clay was observed. Lotierzo and Bon[170] investigated the Pickering miniemulsion polymerization of MMA in the presence of silica nanoparticles (Ludox TM-40), presenting several key insights. They demonstrated that the adhesion of silica nanoparticles to emulsified MMA droplets was not spontaneous, likely due to an electrostatic barrier to adsorption.[171] The mechanism for silica particles ultimately attaching to the interface of a polymer particle was attributed to a heterocoagulation mechanism,[13,41] involving an aqueous phase oligomeric radical growing on the surface of a silica particle. Similar to the results from Brunier *et al.* with LAPONITE® RDS, the polymerization rate increased with increasing the initial concentration of silica, with a greater number of nucleated polymer particles forming upon increasing the concentration of Pickering stabilizer.

"Armoured" particles prepared by Pickering emulsion polymerization have found unique materials applications. A recent example was presented by Delafresnaye *et al.*, who described the preparation of vinylidene chloride (VDC)-based copolymer particles stabilized by clay platelets.[31] PVDC has excellent barrier properties (*e.g.* low oxygen and water permeability) but suffers from processability issues due to its high crystallinity; exfoliated clay platelets also improve barrier properties when present in polymer films. In their work, LAPONITE® S482 clay platelets (1–15% w/w with respect to monomer) were used as Pickering stabilizers of the emulsion polymerization of VDC and methyl acrylate (MA), with MA present from 7 to 17% w/w (total monomer) to ensure that the latex was film-forming. High resolution TEM revealed the targeted armoured particle morphology (Fig. 7, top), with the resulting films exhibiting a honeycomb-like structure due to the confinement of clay platelets within the particle interstices. It was shown that if the VDC content was too high (>87% w/w), the composite films were hard and brittle and cracked easily, whereas optimization of the particle composition gave optically transparent, continuous films at room temperature (Fig. 7, bottom).

Encapsulation using living oligomers

The encapsulation of organic or inorganic materials *via* emulsion polymerization was, for a long time, a challenging question that proved difficult to address. "Armoured" particles (or

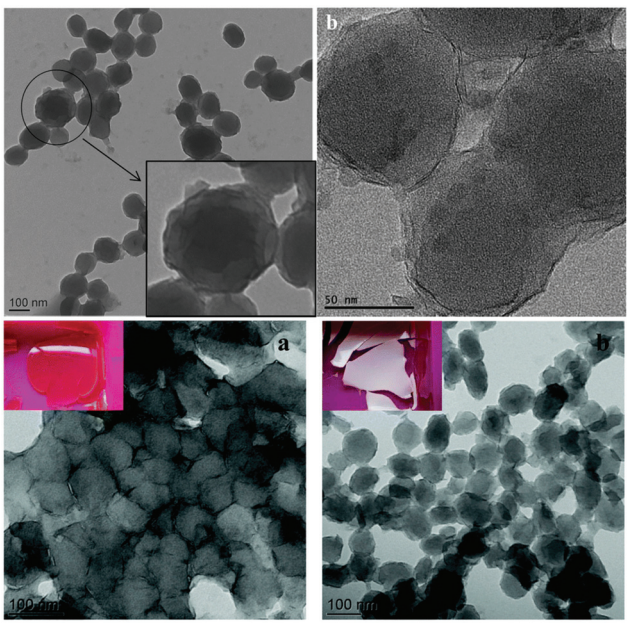

Fig. 7 Poly(VDC-*co*-MA) latexes prepared by Pickering emulsion polymerization with LAPONITE® S482 Clay platelets. Top: TEM and HR-TEM images of 90/10 VDC/MA polymer particles demonstrating clay platelets at the particle interface. Bottom: TEM images and optical photographs of poly(VDC-*co*-MA)/LAPONITE® nanoparticles (10% w/w LAPONITE® relative to monomer) and their resulting films. When the MA content was 15% (A) a transparent uniform film formed, whereas at 10% MA (B) the sample was opaque, brittle and cracked easily. Reproduced from ref. 31 with permission from The Royal Society of Chemistry, copyright 2017.

coagulation) would often result when unmodified nanomaterials were used,[96,172] while the surface modification/hydrophobization approach so readily used in miniemulsion systems is not suitable in emulsion polymerization, given the differences in particle formation mechanism (*i.e.* droplet nucleation *vs.* micellar or homogeneous nucleation).

The successful implementation of RDRP methods in emulsion polymerization in the early 2000's has since paved the way for the encapsulation of nanomaterials *via* the use of amphiphilic living oligomers.[173–181] This has been achieved mostly *via* RAFT emulsion polymerization (often referred to as RAFT-assisted encapsulating emulsion polymerization, or REEP), however examples using NMP[182,183] and ATRP[184–187] have also been demonstrated. The range of nanomaterials that have been encapsulated is remarkably diverse, including silica,[183,188] titania,[173,179] various clays,[174,178,189] quantum dots,[175] carbon nanotubes,[176,177] graphene oxide,[180] layered double hydroxides[189,190] and ceria.[23,191,192] While naturally there are differences in the design of the oligomeric species used, the generic mechanism is the same; an amphiphilic oligomer (*e.g.* a copolymer of *n*-butyl acrylate and acrylic acid) bearing a RAFT end-group undergoes physisorption to the surface of the nanomaterial dispersed in water, followed by starved-feed RAFT emulsion polymerization. Chain extension of the living oligomers results in particle formation occurring around the nanomaterial, providing effective encapsulation even for materials with high aspect ratios. This process is schematically depicted in Fig. 8.

The living oligomers used for successful encapsulation by emulsion polymerization share several common characteristics. Most notably they are amphiphilic in nature and are prepared as random copolymers of hydrophilic and hydrophobic units. A blocky structure is less desirable, as self-assembly can occur in the aqueous phase that may lead to secondary nucleation. The oligomers must also strongly interact with the surface of the nanoparticle, which is readily verified by adsorption isotherm studies. Insufficient surface interaction, or similarly excess oligomer to coat the nanoparticle surface, will again result in oligomers being present in the aqueous phase that can mediate new particle formation. The oligomers also need to be of sufficiently high molecular weight to provide colloidal stability for the resulting latex.

The group of Heuts[187] has recently produced a simple mathematical model to describe the amount of oligomer required to effectively stabilize clay (Gibbsite) platelets and ultimately the final composite latex after starved-feed emulsion polymerization. A particular focus of this work was to determine conditions where both the inorganic filler content and the total polymer solids content were maximized without compromising colloidal stability. In order to achieve very high filler loadings (*e.g.* 40% w/w clay relative to polymer) and high total solids content, an additional feed of oligomer was required later in the reaction, deliberately delayed in order to avoid secondary nucleation early in the reaction profile. Using this strategy, fully encapsulated Gibbsite up to a loading of 20% w/w was achieved within an MMA/BA latex (Fig. 9), with multiple platelets per particle at higher loadings.

Some of the most recent work using the REEP approach has involved the encapsulation of layered double hydroxides (LDHs),[189,190] which are clays of tuneable composition that find use in fire-retardant materials and mechanical reinforcement. The role of the nature of the oligomer and the resulting particle morphology is exemplified. RAFT co-oligomers of acrylic acid and BA (either 15 or 35 total repeat units) were first adsorbed onto the surface of LDH platelets, followed by the starved feed emulsion polymerization of an 80 : 20 mixture of MMA : BA at an LDH loading of 16% w/w. The shorter oligo-

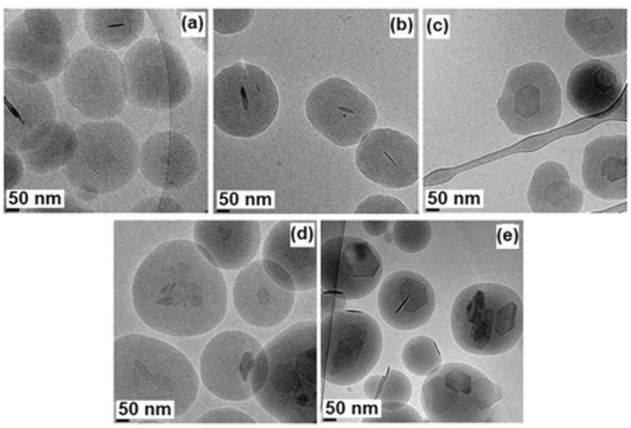

Fig. 9 Poly(MMA-*co*-BA) latexes prepared by starved feed emulsion polymerization in the presence of Gibbsite platelets initially stabilized by (BA4-*co*-AA8 oligomers. Shown are TEM images of nanoparticles prepared at a) 3% (b) 7% (c) 10% (d) 20% and (e) 35% w/w Gibbsite relative to the polymer phase. Samples (c)–(e) were prepared with an additional feed of oligomers during polymerization to impart sufficient colloidal stability. Reproduced with permission from ref. 180. Copyright 2017, John Wiley and Sons.

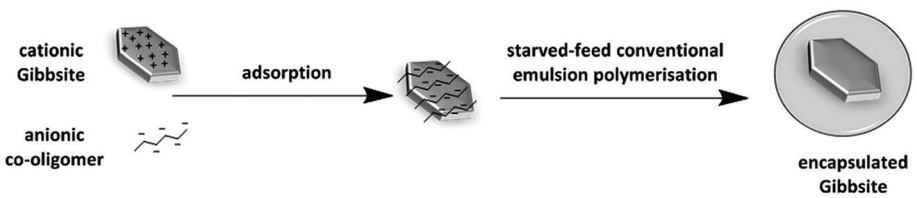

Fig. 8 Schematic process for the encapsulation of inorganic nanoparticles (depicted here for Gibbsite platelets) with living oligomers, prior to starved feed emulsion polymerization. Reproduced from ref. 184 with permission from The Royal Society of Chemistry, copyright 2016.

mers resulted in full encapsulation of the LDH platelets, whereas the longer oligomers gave nanoparticles with a sandwich-type structure. Highlighting the role of the RAFT end group and effective chain extension, the equivalent oligomers with the thiocarbonylthio group removed resulted in the production of armoured particles. When cast as nanocomposite films, highly different mechanical properties were observed; full encapsulation of LDH platelets gave significant mechanical reinforcement relative to the soft polymer matrix. By contrast, the armoured morphology gave a large rubber modulus plateau up to very high temperatures due to the LDH platelets exclusively residing at the particle interface, resulting in a highly percolated network.

Polymerization-induced self-assembly (PISA)

Over the past decade, the method coined *polymerization-induced self-assembly* (PISA) has been an area of intense research interest toward the design of block copolymer nanoparticles of various morphologies at high solids.[193–197] PISA utilizes the ability to readily prepare block copolymers *via* one of the major RDRP methods (*e.g.* RAFT, ATRP and NMP) however the synthetic process is no longer performed in a medium that solubilizes all blocks; in a PISA system, the first block is solvophilic while the second (and subsequent blocks) are solvophobic, resulting in *in situ* assembly (Fig. 10). PISA systems are typically performed as either dispersion or emulsion polymerizations (depending on the monomer solubility in the reaction medium), whereby an increase in the degree of polymerization (DP) of the solvophobic block changes the block copolymer architecture in a continuous fashion, driving self-assembly and the resulting particle morphology.

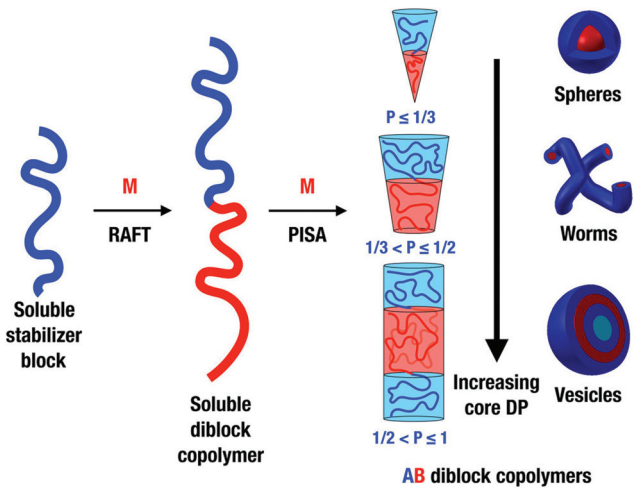

Fig. 10 Schematic overview of the PISA process for the formation of diblock copolymer nanoparticles of varying morphology. Reproduced from S. L. Canning, G. N. Smith and S. P. Armes, *Macromolecules*, 2016, **49**, 1985–2001, published under a Creative Commons Attribution (CC-BY) Licence.

Arguably the most important advantages of the PISA process are predictive morphology control and the retention of "livingness" of a growing polymer chain. The block copolymers prepared by the PISA method self-assemble into nanostructures that are well predicted by the self-assembly of amphiphilic molecules, such as spheres, cylinders/rods, vesicles and lamellae.[198,199] The well-documented morphological evolution in PISA systems (from high curvature to low curvature structures) enables predictive phase diagrams to be prepared based on copolymer composition, solvent and solids content, amongst other factors.[200–208] The PISA process has been extensively reviewed elsewhere;[46,195,196,209] for the scope of this review we address what we believe is an emerging research area, namely colloidal nanocomposites *via* the PISA process. To our knowledge, the *direct* preparation of hybrid nanoparticles *via* the PISA method is particularly small – the use of a methacrylic-functional polyhedral oligomeric silsesquioxane (POSS) derivative as a macroRAFT agent for the dispersion polymerization of styrene in *n*-octane is held up as an example.[210] PISA as an encapsulation methodology or structure-directing method for the preparation of nanocomposites is significantly more common and discussed below.

PISA-based scaffolds for nanocomposite synthesis

One method where colloidal nanocomposites of various morphologies can be prepared is *via* the PISA process as a "colloidal scaffold" amenable to further functionalization. In this approach, block copolymer nanoparticles of targeted morphology are first prepared whereby the solvophilic (or interfacial block) can, for example, act as a chelating agent,[211,212] provide electrostatic attraction,[4] or act as a reactive precursor for interfacial sol–gel synthesis.[213] This two-step approach (particle synthesis followed by functionalization) allows for precise morphological control (*e.g.* vesicles or fibres) prior to any modification steps that may compromise the targeted morphology.

Examples of this approach were reported by the groups of Davis and Boyer, who used RAFT dispersion polymerization in methanol to prepare block copolymer nanoparticles where both iron oxide and gold nanoparticles could be nucleated and stabilized at the particle interface.[211,212] Triblock copolymers were prepared using an oligo (ethylene glycol) methacrylate (OEGMA)-based macroRAFT agent, where chain extension was first performed in solution either with MAA (in methanol) or 2-(*N*,*N*-dimethylamino)ethyl methacrylate (DMAEMA) (in toluene), followed by PISA of St in methanol. In both cases the [St] : [macroRAFT] ratio in the PISA step was particularly high (5000), analogous to the "monomer flooded" PISA approach of Pan's group.[214,215] In both cases, triblock copolymers of composition OEGMA-*b*-MAA-*b*-St or OEGMA-*b*-DMAEMA-*b*-St were formed with moderate dispersity (1.28–1.72 and 1.30–1.45 respectively) that self-assembled into spheres, worms and vesicles as a function of the DP of the St block. MAA-functional particles were dialyzed against water and the pendant carboxylic acid groups were used to complex a 1 : 2 mixture of Fe(II) : Fe(III) salts that were precipitated with excess base to form nanoparticles 7–10 nm in diameter. An analogous

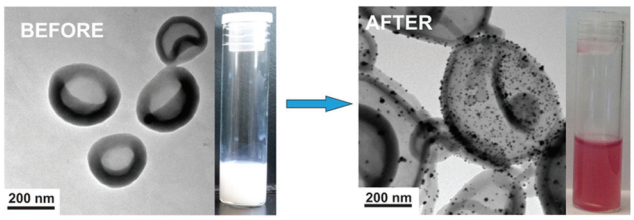

Fig. 11 TEM images and optical micrographs of poly(OEGMA-*b*-DMAEMA-*b*-St) vesicles prepared by the PISA in methanol, before and after complexation of the tertiary amine groups with chloroauric acid and subsequent reduction with $NaBH_4$ to form gold nanoparticles. Reprinted with permission from R. Bleach, B. Karagoz, S. M. Prakash, T. P. Davis and C. Boyer, *ACS Macro Lett.*, 2014, **3**, 591–596. Copyright 2014 American Chemical Society.

approach was used with DMAEMA-functionalized nanoparticles, used to complex chloroauric acid before chemical reduction to yield stable Au nanoparticles of similar diameter (Fig. 11). Polymeric spheres, rods and vesicles were all able to be decorated *via* this approach, importantly resulting in no loss of colloidal stability or affecting the particle size/morphology of the polymer scaffolds. The iron oxide nanoparticle-functional scaffolds were shown to be effective MRI relaxation agents, with the micellar morphology shown to be the most effective in this context.

The decoration of polymeric nanofibres prepared by RAFT emulsion polymerization with pre-formed iron oxide nanoparticles was recently reported by Nguyen *et al.*[4] In their approach, a symmetric RAFT agent was used to prepare an AA-*b*-BA-*b*-St triblock copolymer in 1,4-dioxane (relative M_n = 20 kDa, $Đ$ = 1.20) that served as a polymeric stabilizer for the emulsion polymerization of styrene in water, with [St] : [triblock] ratios varying from 660 to 2220. Moderate to high conversions (>82%) were reported in all cases, with spheres, fibres, platelets and vesicular structures reported. The targeted fibrous structure, carrying an inherent negative charge from the presence of AA groups at the surface (zeta potential = −50 mV at pH 7.5) was blended with a 4% w/w dispersion of pre-formed iron oxide particles (particle size 25 nm); the positive surface charge on the iron oxide was used to create a composite *via* electrostatic attraction. The resulting composite was ~51% w/w iron oxide, with the resulting fibres aligning under an applied external magnetic field.

Our contribution to this area has involved the synthesis of polymer/silica colloidal nanocomposites of various morphologies *via* the combination of PISA and sol–gel chemistry.[213] A reactive alkoxysilane-based methacrylate (MPS) was used as the solvophilic block for the RAFT dispersion polymerization of benzyl methacrylate (BzMA) in ethanol; the resulting particles (spheres and vesicles) were used as scaffolds to direct the base-catalyzed condensation of a silica precursor (TEOS) at the particle interface. Silica shells of uniform thickness (~40 nm) were formed at the particle surface by feeding in the TEOS precursor slowly to minimize secondary nucleation with preservation of the initial particle morphology. Typical of RAFT dispersion polymerization systems, the degree of polymerization of the solvophilic block played a key role in directing particle morphology – transitions from spheres through to vesicles were observed when the MPS block was relatively short (40 units), whereas spherical nanoparticles were exclusively observed when the MPS stabilizer was 65 units in length, preventing effective particle rearrangement.[195]

In situ encapsulation during the PISA process

The ability of the PISA process to readily prepare polymeric vesicles (also referred to as 'polymersomes') at high solids has been exploited in the past few years to investigate the loading of vesicles with inorganic nanoparticles and proteins. The use of vesicles is particularly appealing in the context of microencapsulation for various chemical or biomedical applications,[216–219] in particular if the payload encapsulated within the vesicle can be readily released *via* disruption of the vesicle membrane.

The group of Armes has made significant advances in understanding the mechanism of encapsulation and release of silica nanoparticles from polymeric vesicles in aqueous solution.[220–222] Diblock copolymer vesicles were prepared by the RAFT aqueous dispersion polymerization of 2-hydroxypropyl methacrylate (HPMA), using a glycerol monomethacrylate (GMA) macroRAFT agent. The unusual properties of HPMA, namely the monomer being water soluble but the resultant polymer being insoluble, enables a dispersion polymerization mechanism to be employed. A typical diblock composition to yield a vesicular structure was GMA_{58}-*b*-$HPMA_{250}$, prepared at relatively low dispersity (*circa* 1.12). The loading of 18 nm silica nanoparticles into these vesicles was first achieved by performing the PISA process in the presence of the silica dispersion, at silica loadings up to 35% w/w, followed by multiple centrifugation cycles to remove non-encapsulated silica.[222] Disk centrifuge photosedimentometry (DCP) was used to demonstrate a loading of over 100 silica nanoparticles per vesicle at the highest silica loading, with loading efficiencies (by TGA) of approximately 10%. As the HPMA block is thermoresponsive, time-resolved SAXS and TEM were used to demonstrate a vesicle-to-sphere morphology transition (and accompanying release of silica nanoparticles) upon cooling the loaded vesicles from 30 °C to 0 °C; the transition was deemed complete in approximately 12 minutes. A similar encapsulation and release mechanism was demonstrated for polymeric vesicles loaded with bovine serum albumin (BSA). A subsequent paper from the group showed that vesicles with a high initial silica loading dissociate *via* a "membrane perforation" mechanism as studied by time-resolved SAXS, as opposed to the vesicle-to-sphere morphology change at lower loadings.[221]

In addition to thermally driven morphological changes to drive payload release, Armes' group has utilized dynamic covalent chemistry to release silica nanoparticles from the interior of a polymer vesicle *via* an *order-order* transition.[220] 3-Aminophenylboronic acid (APBA) was added to GMA-*b*-HPMA vesicles described above at pH 10, which drove a small but significant increase in the volume fraction of the stabilizer block *via* the formation of borate ester groups through reaction

with the *cis*-diol groups of GMA.[223] The addition of ABPA resulted in vesicle rearrangement into polymeric worms whereby the silica payload was released (Fig. 12); the rate of rearrangement could be tuned by adjusting the ABPA concentration of the pH of the aqueous medium. Importantly, this methodology enables the release of encapsulated nanoparticles from vesicles where a thermoresponsive transition would not be possible, such as thick-walled vesicles.[224,225]

A further approach towards the realization of silica-loaded vesicles has been reported by the group of Li Zhang, whereby aqueous RAFT dispersion polymerization was performed using photoinitiation using 405 nm light.[226,227] A PEG-based macroRAFT agent was used to mediate the chain extension of HPMA in water at solids content of 10% w/w, using the water soluble photoinitiator sodium phenyl-2,4,6-trimethylbenzoylphosphinate (SPTP). A clear advantage of this photoPISA approach is the rapid reaction times-compared to thermal initiation; the preparation of vesicles of composition PEG_{113}-*b*-$HPMA_{400}$ was shown to be complete after only 15 minutes of irradiation, with the polymer exhibiting low dispersity ($Đ$ = 1.27). This compared to >2 h to reach full conversion using thermal initiation. PhotoPISA in the presence of a commercial aqueous dispersion of silica nanoparticles (LUDOX AM) at 30% w/w resulted in silica loaded vesicles whereby TEM analysis revealed silica particles in the vesicle interior as well as the walls of the membrane. Polymer vesicles that were able to disassemble were also prepared by the photoPISA of a 9 : 1 mol : mol mixture of HPMA and DMAEMA in water, yielding vesicles that dissociated upon bubbling CO_2 into the reaction mixture, increasing the hydrophilicity of the core-forming block and driving disassembly.[226]

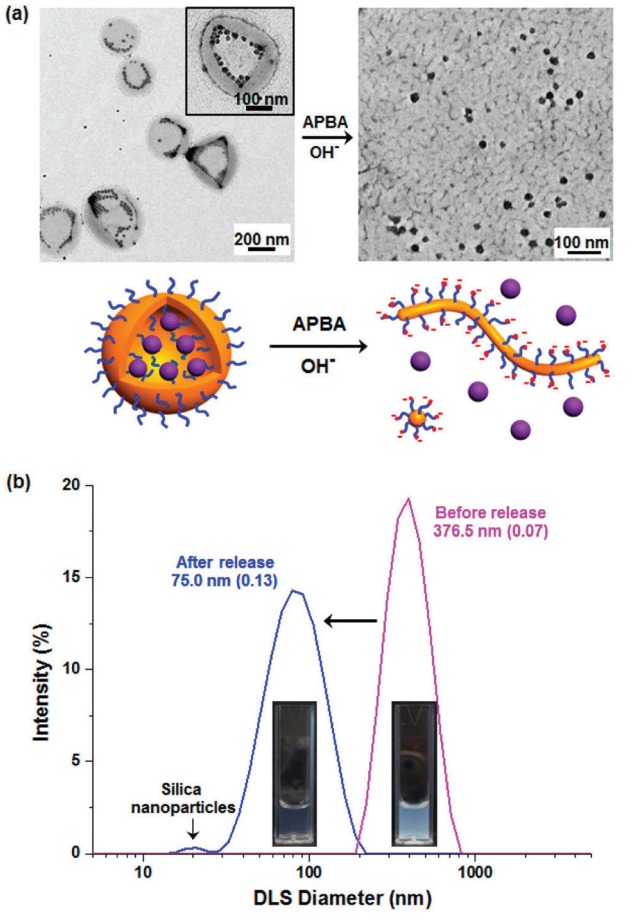

Fig. 12 Encapsulation and release from polymeric vesicles *via* order-order transitions. TEM images (a) and DLS distributions (b) of GMA-*b*-HPMA vesicles prepared by PISA loaded with silica nanoparticles. The addition of ABPA induces a vesicle-to-worm transition and subsequent release of the encapsulated silica. Reproduced from R. Deng, M. J. Derry, C. J. Mable, Y. Ning and S. P. Armes, *J. Am. Chem. Soc.*, 2017, **139**, 7616–7623, published under a Creative Commons Attribution (CC-BY) Licence.

PISA from nanoparticle surfaces

Examples of polymer-silica colloidal nanocomposites have been prepared using polymerization-induced self-assembly (PISA) directly from the surface of a silica nanoparticle. The group of Benicewicz[228,229] has recently used surface-initiated PISA to create polymer-silica nanoparticle strings and vesicles. Their approach used silica nanoparticles of diameter ~15 nm functionalized with the RAFT agent 2-cyano-2-propyl benzodithioate (CPDB) in order to grow chains of poly(2-hydroxyethyl methacrylate) poly(HEMA) with DP = 190 followed by removal of the RAFT end-group; the purpose of this step was to provide a layer of solvophilic polymer grafted to the surface to provide colloidal stability in methanol. A second round of RAFT surface modification was followed by the RAFT dispersion polymerization of BzMA in methanol, forming a "mixed brush" surface of solvophilic and solvophobic homopolymers. Similar to a classical PISA experiment, the solution moved from transparent to turbid and ultimately milky-white in appearance with increasing fractional conversion of BzMA, coupled with an increase in hydrodynamic diameter by DLS (from 28 nm to over 200 nm). TEM analysis revealed the formation of short strings of nanoparticles, driven by mixing of the grafted solvophobic brushes. Analogous experiments with poly(HPMA) as the stabilizer block, followed by the surface initiated dispersion polymerization of BzMA in ethanol resulted in the formation of single-walled hybrid vesicles.

Another approach demonstrating surface-initiated PISA was reported by the group of Bourgeat-Lami,[182] where NMP was used to mediate the emulsion copolymerization of butyl methacrylate and styrene. In this work, a macroalkoxyamine was first prepared (poly(OEGMA$_{12}$-*co*-St$_1$), M_n = 11.7 kDa, $Đ$ = 1.11) and then added to an acidified aqueous dispersion of silica nanoparticles (diameter 136 nm), enabling physisorption of the macroalkoxyamine at the silica nanoparticle interface. Subsequent emulsion polymerization of a BMA/St mixture resulted in composite particles of varying morphology; these included core–shell and "half-capped" spheres, tadpole-like and snowman-vesicles that formed at different pH of the continuous phase. A strong dependence on the size of the silica nanoparticles was also reported; when much smaller silica nanoparticles (~30 nm diameter) were used, "armoured" fibres and vesicles were instead formed.

Table 1 Summary of design considerations in preparing colloidal nanocomposites of specific morphology by the techniques discussed in this article

Target morphology	Miniemulsion polymerization	Emulsion polymerization	Polymerization-induced self-assembly
Encapsulated	Surface modification of (in)organic phase typically required for dispersal in monomer phase Hollow particles or capsules are possible Need to consider interfacial tension terms to achieve target	Amphiphilic living oligomer needed for stabilization of (in)organic phase and particle nucleation and growth High aspect ratio and anisotropic materials can be encapsulated Scalable approach compared to miniemulsion	*In situ* encapsulation of nanoparticles is possible but encapsulation efficiency can be low Higher order morphologies (rods, worms, vesicles) are readily accessed
"Armoured"	Surface modification of (in)organic phase not essential, but particles need to wet droplet interface Droplet nucleation simplifies particle design	Complete mechanism of particle formation is still emerging Particle adsorption at latex interface is highly system dependent, often many "bare" particles	PISA nanoparticles can be used as a reactive scaffold for surface modification Surface modification is independent of polymer nanoparticle morphology

Conclusions and outlook

The past decade has seen extensive development in colloidal nanocomposite synthesis through a variety of heterogeneous polymerization methods. Major shortcomings have been overcome, such as the ability to encapsulate unmodified (in)organic nanoparticles *via* emulsion polymerization *via* the "REEP" approach, through the use of living amphiphilic oligomers to adsorb to the surface of the encapsulation target. This has, in our opinion, tipped the balance away from miniemulsion polymerization as the method of choice for particle encapsulation, given that potentially laborious and/or inefficient surface modification of the nanomaterial is required for miniemulsion polymerization. The applicability of emulsion polymerization on an industrial and commercial scale makes this method even more attractive. The use of miniemulsion polymerization naturally retains some technical advantages, in particular the design of hollow particles and polymeric capsules with an encapsulated payload, and the relative simplicity of droplet nucleation. Table 1 summarizes some of the key design considerations of the approaches discussed in this article with respect to armoured or encapsulated morphologies.

The advent of PISA, particularly all-aqueous PISA, has revolutionized the ability to prepare polymeric nanoparticles of diverse morphologies at high solids. "Non-traditional" morphologies such as worms/rods and vesicles have potential application in numerous settings, such as novel materials for encapsulation and release as highlighted in this article. The *in situ* encapsulation within the interior of polymeric vesicles is remarkably simple to perform, and has provided exciting developments into the mechanism of payload release when a vesicle undergoes dissociation. This method suffers from a potentially large fraction of unencapsulated nanoparticles, in addition to distribution of encapsulated nanoparticles per vesicle that is not readily controlled. We anticipate that the ability to address these issues will be areas of active research in coming years.

Pickering miniemulsion and emulsion polymerization have also seen extensive development in recent years, both from a mechanistic and applied perspective. The appeal of particle-based stabilizers is immediate, as it circumvents the need for low molecular weight surfactants which is particularly appealing for film-forming latexes. The resulting "armoured" or raspberry-type morphology sees numerous applications in the context of reactive surface coatings or materials with unique mechanical response. Ensuring that nanoparticles are adsorbed at the monomer droplet/polymer particle interface often requires fine control of the monomer composition, including the use of auxillary comonomers, and control of the pH and ionic strength of the continuous phase. The knowledge that has been developed in this area in recent times will further enable the design of well-controlled nanomaterials for specific applications.

In conclusion, this is an exciting time to be working in the area of colloidal nanocomposites. The underlying knowledge with respect to encapsulation as well as particle-based stabilization in heterogeneous polymerization has grown extensively, and this knowledge will undoubtedly feed further developments in materials applications such as surface coatings with tailored function. We envisage the use of bio-based and naturally derived materials in colloidal nanocomposite preparation to grow significantly, given the social and economic drivers for sustainability in chemistry and materials science. The potential for applications in other areas such as catalysis and nanomedicine, amongst others, will ensure that colloidal nanocomposites remain an active area of research for many years to come.

Abbreviations

4VP	4-Vinylpyridine
AA	Acrylic acid
APBA	3-Aminophenylboronic acid
ATRP	Atom transfer radical polymerization
BA	*n*-Butyl acrylate
BMEP	[2-(Methacryloyloxy)ethyl] phosphate
BzMA	Benzyl methacrylate
CNC	Cellulose nanocrystal

CNF	Cellulose nanofibre
CTAB	Cetyltrimethylammonium bromide
$Đ$	Dispersity
DMAEMA	2-(*N*,*N*-Dimethylamino)ethyl methacrylate
DP	Degree of polymerization
DVB	Divinylbenzene
EGDMA	Ethylene glycol dimethacrylate
GMA	Glycerol monomethacrylate
GO	Graphene oxide
HEMA	2-Hydroxyethyl methacrylate
HPMA	2-Hydroxypropyl methacrylate
LDH	Layered double hydroxide
MA	Methyl acrylate
MDI	Methylene diphenyl diisocyanate
MMA	Methyl methacrylate
MMT	Montmorillonite
M_n	Number average molar mass
MPS	3-(Trimethoxysilyl)propyl methacrylate
NMP	Nitroxide mediated polymerization
OA	Oleic acid
OEGMA	Oligo(ethylene glycol) methacrylate
PEG	Polyethylene glycol
PISA	Polymerization-induced self-assembly
RAFT	Reversible addition fragmentation chain transfer
RDRP	Reversible deactivation radical polymerization
REEP	RAFT-assisted encapsulating emulsion polymerization
SDBS	Sodium dodecyl benzenesulfonate
SDS	Sodium dodecyl sulfate
SEM	Scanning electron microscopy
St	Styrene
TBT	Tetra *n*-butyltitanate
TEM	Transmission electron microscopy
TEOS	Tetraethylorthosilicate
T_g	Glass transition temperature
VBDAC	Vinylbenzyldodecyltrimethylammonium chloride
VDC	Vinylidene chloride

Conflicts of interest

There are no conflicts to declare.

Acknowledgements

GHT acknowledges the provision of a post-graduate scholarship from the University of Tasmania.

Notes and references

1 M. Errezma, A. B. Mabrouk and S. Boufi, *Prog. Org. Coat.*, 2017, **109**, 30–37.
2 S. Kalele, S. W. Gosavi, J. Urban and S. K. Kulkarni, *Curr. Sci.*, 2006, **91**, 1038–1052.
3 E. González, A. Bonnefond, M. Barrado, A. M. Casado Barrasa, J. M. Asua and J. R. Leiza, *Chem. Eng. J.*, 2015, **281**, 209–217.
4 D. Nguyen, V. Huynh, N. Pham, B. Pham, A. Serelis, T. Davey, C. Such and B. Hawkett, *Macromol. Rapid Commun.*, 2018, 1800402.
5 E. Bourgeat-Lami, T. R. Guimarães, A. M. C. Pereira, G. M. Alves, J. C. Moreira, J.-L. Putaux and A. M. dos Santos, *Macromol. Rapid Commun.*, 2010, **31**, 1874–1880.
6 A. Bonnefond, M. Paulis, S. A. F. Bon and J. R. Leiza, *Langmuir*, 2013, **29**, 2397–2405.
7 J. A. Balmer, A. Schmid and S. P. Armes, *J. Mater. Chem.*, 2008, **18**, 5722–5730.
8 E. Bourgeat-Lami, *J. Nanosci. Nanotechnol.*, 2002, **2**, 1–24.
9 E. Bourgeat-Lami and M. Lansalot, *Adv. Polym. Sci.*, 2010, **233**, 53–123.
10 K. Landfester, *Angew. Chem., Int. Ed.*, 2009, **48**, 4488–4507.
11 K. Y. van Berkel and C. J. Hawker, *J. Polym. Sci., Part A: Polym. Chem.*, 2010, **48**, 1594–1606.
12 D. Qi, Z. Cao and U. Ziener, *Adv. Colloid Interface Sci.*, 2014, **211**, 47–62.
13 N. Sheibat-Othman and E. Bourgeat-Lami, *Langmuir*, 2009, **25**, 10121–10133.
14 E. Bourgeat-Lami, I. Tissot and F. Lefebvre, *Macromolecules*, 2002, **35**, 6185–6191.
15 M. Kim, Y. K. Kim, J. Kim, S. Cho, G. Lee and J. Jang, *RSC Adv.*, 2016, **6**, 27460–27465.
16 H. Zhu, Q. Zhang and S. Zhu, *Dalton Trans.*, 2015, **44**, 16752–16757.
17 J.-F. Dechezelles, V. Malik, J. J. Crassous and P. Schurtenberger, *Soft Matter*, 2013, **9**, 2798–2802.
18 J. Moraes, K. Ohno, T. Maschmeyer and S. Perrier, *Chem. Commun.*, 2013, **49**, 9077–9088.
19 S. F. Medeiros, A. M. Santos, H. Fessi and A. Elaissari, *J. Colloid Sci. Biotechnol.*, 2012, **1**, 99–112.
20 F. Zhang, S. Yu, G. Hou, N. Xu, Z. Wu and L. Yue, *Colloid Polym. Sci.*, 2015, **293**, 1893–1902.
21 S. Chakraborty, K. Jähnichen, H. Komber, A. A. Basfar and B. Voit, *Macromolecules*, 2014, **47**, 4186–4198.
22 C. Kaewsaneha, P. Tangboriboonrat, D. Polpanich, M. Eissa and A. Elaissari, *J. Polym. Sci., Part A: Polym. Chem.*, 2013, **51**, 4779–4785.
23 J. Warnant, J. Garnier, A. van Herk, P.-E. Dufils, J. Vinas and P. Lacroix-Desmazes, *Polym. Chem.*, 2013, **4**, 5656–5663.
24 T. Chen, P. J. Colver and S. A. F. Bon, *Adv. Mater.*, 2007, **19**, 2286–2289.
25 T. de Roo, S. Huber and S. Mecking, *ACS Macro Lett.*, 2016, 786–789, DOI: 10.1021/acsmacrolett.6b00323.
26 M. Dinari, M. M. Momeni and M. Goudarzirad, *Surf. Eng.*, 2016, **32**, 535–540.
27 A. Fokina, K. Klinker, L. Braun, B. G. Jeong, W. K. Bae, M. Barz and R. Zentel, *Macromolecules*, 2016, **49**, 3663–3671.
28 S. A. F. Bon and P. J. Colver, *Langmuir*, 2007, **23**, 8316–8322.

29 B. Brunier, N. Sheibat-Othman, M. Chniguir, Y. Chevalier and E. Bourgeat-Lami, *Langmuir*, 2016, **32**, 6046–6057.
30 A. Chakrabarty, L. Zhang, K. A. Cavicchi, R. A. Weiss and N. K. Singha, *Langmuir*, 2015, **31**, 12472–12480.
31 L. Delafresnaye, P.-Y. Dugas, P.-E. Dufils, I. Chaduc, J. Vinas, M. Lansalot and E. Bourgeat-Lami, *Polym. Chem.*, 2017, **8**, 6217–6232.
32 E. Zengeni, P. C. Hartmann and H. Pasch, *ACS Appl. Mater. Interfaces*, 2012, **4**, 6957–6968.
33 T. Kuilla, S. Bhadra, D. Yao, N. H. Kim, S. Bose and J. H. Lee, *Prog. Polym. Sci.*, 2010, **35**, 1350–1375.
34 A. Y. W. Sham and S. M. Notley, *Soft Matter*, 2013, **9**, 6645–6653.
35 E. Bourgeat-Lami, J. Faucheu and A. Noel, *Polym. Chem.*, 2015, **6**, 5323–5357.
36 H. Kim, A. A. Abdala and C. W. Macosko, *Macromolecules*, 2010, **43**, 6515–6530.
37 D. R. Wang, G. Ye, X. L. Wang and X. G. Wang, *Adv. Mater.*, 2011, **23**, 1122–1125.
38 H. M. Etmimi and R. D. Sanderson, *Macromolecules*, 2011, **44**, 8504–8515.
39 H. M. Etmimi, M. P. Tonge and R. D. Sanderson, *J. Polym. Sci., Part A: Polym. Chem.*, 2011, **49**, 1621–1632.
40 S. C. Thickett, N. Wood, Y. H. Ng and P. B. Zetterlund, *Nanoscale*, 2014, **6**, 8590–8594.
41 S. C. Thickett and P. B. Zetterlund, *ACS Macro Lett.*, 2013, **2**, 630–634.
42 J.-M. Thomassin, M. Trifkovic, W. Alkarmo, C. Detrembleur, C. Jérôme and C. Macosko, *Macromolecules*, 2014, **47**, 2149–2155.
43 V. H. Pham, T. T. Dang, S. H. Hur, E. J. Kim and J. S. Chung, *ACS Appl. Mater. Interfaces*, 2012, **4**, 2630–2636.
44 N. Park, J. Lee, H. Min, Y. D. Park and H. S. Lee, *Polymer*, 2014, **55**, 5088–5094.
45 J. K. Oh, *J. Polym. Sci., Part A: Polym. Chem.*, 2008, **46**, 6983–7001.
46 P. B. Zetterlund, S. C. Thickett, S. Perrier, E. Bourgeat-Lami and M. Lansalot, *Chem. Rev.*, 2015, **115**, 9745–9800.
47 P. B. Zetterlund, Y. Kagawa and M. Okubo, *Chem. Rev.*, 2008, **108**, 3747–3794.
48 M. Save, Y. Guillaneuf and R. G. Gilbert, *Aust. J. Chem.*, 2006, **59**, 693–711.
49 C. K. Weiss and K. Landfester, in *Hybrid Latex Particles: Preparation with (Mini)emulsion Polymerization*, ed. A. M. van Herk and K. Landfester, Springer Berlin Heidelberg, Berlin, Heidelberg, 2010, pp. 185–236, DOI: 10.1007/12_2010_61.
50 K. Landfester and V. Mailänder, *Expert Opin. Drug Delivery*, 2013, **10**, 593–609.
51 J. M. Asua, *Prog. Polym. Sci.*, 2002, **27**, 1283–1346.
52 M. Antonietti and K. Landfester, *Prog. Polym. Sci.*, 2002, **27**, 689–757.
53 Z. Cao, Q. Chen, H. Chen, Z. Chen, J. Yao, S. Zhao, Y. Zhang and D. Qi, *Colloids Surf., A*, 2017, **516**, 199–210.
54 K. Landfester, in *Colloid Chemistry II*, ed. M. Antonietti, Springer, Berlin Heidelberg, 2003, pp. 75–123, DOI: 10.1007/3-540-36412-9_4.
55 P. Taylor, *Adv. Colloid Interface Sci.*, 1998, **75**, 107–163.
56 M. Aguirre, M. Paulis, M. Barrado, M. Iturrondobeitia, A. Okariz, T. Guraya, J. Ibarretxe and J. R. Leiza, *J. Polym. Sci., Part A: Polym. Chem.*, 2014, **53**, 792–799.
57 J. M. Asua, *Macromol. Chem. Phys.*, 2014, **215**, 458–464.
58 W. Stöber, A. Fink and E. Bohn, *J. Colloid Interface Sci.*, 1968, **26**, 62–69.
59 I. I. Slowing, J. L. Vivero-Escoto, C.-W. Wu and V. S. Y. Lin, *Adv. Drug Delivery Rev.*, 2008, **60**, 1278–1288.
60 S. Zheng, F. Fang, G. Zhou, G. Chen, L. Ouyang, M. Zhu and D. Sun, *Chem. Mater.*, 2008, **20**, 3954–3958.
61 F. Tiarks, K. Landfester and M. Antonietti, *Langmuir*, 2001, **17**, 5775–5780.
62 S.-W. Zhang, S.-X. Zhou, Y.-M. Weng and L.-M. Wu, *Langmuir*, 2005, **21**, 2124–2128.
63 D.-M. Qi, Y.-Z. Bao, Z.-X. Weng and Z.-M. Huang, *Polymer*, 2006, **47**, 4622–4629.
64 X. Qiao, M. Chen, J. Zhou and L. Wu, *J. Polym. Sci., Part A: Polym. Chem.*, 2007, **45**, 1028–1037.
65 J. Zhou, S. Zhang, X. Qiao, X. Li and L. Wu, *J. Polym. Sci., Part A: Polym. Chem.*, 2006, **44**, 3202–3209.
66 E. Bourgeat-Lami, G. A. Farzi, L. David, J. L. Putaux and T. F. L. McKenna, *Langmuir*, 2012, **28**, 6021–6031.
67 A. Mirmohseni, A. Gharieh and M. Khorasani, *Polymer*, 2016, **98**, 182–189.
68 M. Sanei, A. R. Mahdavian, S. Torabi and H. Salehi-Mobarakeh, *Polym. Bull.*, 2017, **74**, 1879–1898.
69 Y. Zhang, Z. Chen, Z. Dong, M. Zhao, S. Ning and P. He, *Int. J. Polym. Mater. Polym. Biomater.*, 2013, **62**, 397–401.
70 A. Schmid, S. P. Armes, C. A. P. Leite and F. Galembeck, *Langmuir*, 2009, **25**, 2486–2494.
71 A. Schmid, P. Scherl, S. P. Armes, C. A. P. Leite and F. Galembeck, *Macromolecules*, 2009, **42**, 3721–3728.
72 A. Schmid, J. Tonnar and S. P. Armes, *Adv. Mater.*, 2008, **20**, 3331–3336.
73 X. Liu, Y. Guan, H. Liu, Z. Ma, Y. Yang and X. Wu, *J. Magn. Magn. Mater.*, 2005, **293**, 111.
74 X. Liu, Y. Guan, Z. Ma and H. Liu, *Langmuir*, 2004, **20**, 10278.
75 S. Lu and J. Forcada, *J. Polym. Sci., Part A: Polym. Chem.*, 2006, **44**, 4187.
76 S. Lu, R. Qu and J. Forcada, *Mater. Lett.*, 2009, **63**, 2539.
77 S. Lu, J. Ramos and J. Forcada, *Langmuir*, 2007, **23**, 12893.
78 S. Lu, J. Ramos and J. Forcada, *Macromol. Symp.*, 2009, **281**, 89.
79 A. R. Mahdavian, M. Ashjari and H. S. Mobarakeh, *J. Appl. Polym. Sci.*, 2008, **110**, 1242.
80 J. S. Nunes, C. L. de Vasconcelos, F. A. O. Cabral, J. H. de Araújo, M. R. Pereira and J. L. C. Fonseca, *Polymer*, 2006, **27**, 7646.
81 B. M. Teo, F. Chen, T. A. Hatton, F. Grieser and M. Ashokkumar, *Langmuir*, 2009, **25**, 2593.

82 V. Holzapfel, M. Lorenz, C. K. Weiss, H. Schrezenmeier, K. Landfester and V. Mailander, *J. Phys.: Condens. Matter*, 2006, **18**, S2581.
83 K. Landfester and L. P. Ramirez, *J. Phys.: Condens. Matter*, 2003, **15**, S1345.
84 L. P. Ramirez and K. Landfester, *Macromol. Chem. Phys.*, 2003, **204**, 22.
85 N. Steiert and K. Landfester, *Macromol. Mater. Eng.*, 2007, **292**, 1111–1125.
86 F. Tiarks, K. Landfester and M. Antonietti, *Macromol. Chem. Phys.*, 2001, **202**, 51–60.
87 E. Zengeni, P. C. Hartmann and H. Pasch, *Macromol. Chem. Phys.*, 2013, **214**, 62–75.
88 J. Ramos and J. Forcada, *Langmuir*, 2011, **27**, 7222–7230.
89 K. Y. van Berkel, A. M. Piekarski, P. H. Kierstead, E. D. Pressly, P. C. Ray and C. J. Hawker, *Macromolecules*, 2009, **42**, 1425.
90 D. Majumdar, T. N. Blanton and D. W. Schwark, *Appl. Clay Sci.*, 2003, **23**, 265–273.
91 T.-K. Oh, M. Hassan, C. Beatty and H. El-Shall, *J. Appl. Polym. Sci.*, 2006, **100**, 3465–3473.
92 T. Sugama, *Mater. Lett.*, 2006, **60**, 2700–2706.
93 N. P. Ashby and B. P. Binks, *Phys. Chem. Chem. Phys.*, 2000, **2**, 5640–5646.
94 S. Cauvin, P. J. Colver and S. A. F. Bon, *Macromolecules*, 2005, **38**, 7887–7889.
95 D. J. Voorn, W. Ming and A. M. van Herk, *Macromolecules*, 2006, **39**, 2137–2143.
96 N. Negrete-Herrera, J.-L. Putaux, L. David, F. D. Haas and E. Bourgeat-Lami, *Macromol. Rapid Commun.*, 2007, **28**, 1567–1573.
97 S. Stankovich, D. A. Dikin, G. H. B. Dommett, K. M. Kohlhaas, E. J. Zimney, E. A. Stach, R. D. Piner, S. T. Nguyen and R. S. Ruoff, *Nature*, 2006, **442**, 282–286.
98 S. Stankovich, D. A. Dikin, R. D. Piner, K. A. Kohlhaas, A. Kleinhammes, Y. Jia, Y. Wu, S. T. Nguyen and R. S. Ruoff, *Carbon*, 2007, **45**, 1558–1565.
99 S. Stankovich, R. D. Piner, X. Q. Chen, N. Q. Wu, S. T. Nguyen and R. S. Ruoff, *J. Mater. Chem.*, 2006, **16**, 155–158.
100 J. Kim, L. J. Cote, F. Kim, W. Yuan, K. R. Shull and J. Huang, *J. Am. Chem. Soc.*, 2010, **132**, 8180–8186.
101 J.-W. Kim, D. Lee, H. C. Shum and D. A. Weitz, *Adv. Mater.*, 2008, **20**, 3239–3243.
102 J. Kim, L. J. Cote and J. Huang, *Acc. Chem. Res.*, 2012, **45**, 1356–1364.
103 L. J. Cote, J. Kim, V. C. Tung, J. Luo, F. Kim and J. Huang, *Pure Appl. Chem.*, 2011, **83**, 95–110.
104 B. Konkena and S. Vasudevan, *J. Phys. Chem. Lett.*, 2012, **3**, 867–872.
105 B. Konkena and S. Vasudevan, *Langmuir*, 2012, **28**, 12432–12437.
106 X. Song, Y. Yang, J. Liu and H. Zhao, *Langmuir*, 2010, **27**, 1186–1191.
107 M. M. Gudarzi and F. Sharif, *Soft Matter*, 2011, **7**, 3432–3440.
108 B. T. McGrail, J. D. Mangadlao, B. J. Rodier, J. Swisher, R. Advincula and E. Pentzer, *Chem. Commun.*, 2016, **52**, 288–291.
109 B. T. McGrail, B. J. Rodier and E. Pentzer, *Chem. Mater.*, 2014, **26**, 5806–5811.
110 B. J. Rodier, A. de Leon, C. Hemmingsen and E. Pentzer, *Polym. Chem.*, 2018, **9**, 1547–1550.
111 B. J. Rodier, E. P. Mosher, S. T. Burton, R. Matthews and E. Pentzer, *Macromol. Rapid Commun.*, 2016, **37**, 894–899.
112 A. C. de Leon, L. Alonso, J. D. Mangadlao, R. C. Advincula and E. Pentzer, *ACS Appl. Mater. Interfaces*, 2017, **9**, 14265–14272.
113 S. H. Che Man, S. C. Thickett, M. R. Whittaker and P. B. Zetterlund, *J. Polym. Sci., Part A: Polym. Chem.*, 2013, **51**, 47–58.
114 S. C. Thickett and P. B. Zetterlund, *J. Colloid Interface Sci.*, 2015, **442**, 67–74.
115 G. H. Teo, Y. H. Ng, P. B. Zetterlund and S. C. Thickett, *Polymer*, 2015, **63**, 1–9.
116 S. H. Che Man, D. Ly, M. R. Whittaker, S. C. Thickett and P. B. Zetterlund, *Polymer*, 2014, **55**, 3490–3497.
117 S. H. Che Man, N. Y. Mohd Yusof, M. R. Whittaker, S. C. Thickett and P. B. Zetterlund, *J. Polym. Sci., Part A: Polym. Chem.*, 2013, **51**, 5153–5162.
118 Y. Fadil, S. H. C. Man, F. Jasinski, H. Minami, S. C. Thickett and P. B. Zetterlund, *J. Polym. Sci., Part A: Polym. Chem.*, 2017, **55**, 2289–2297.
119 A. Fujishima and X. Zhang, *C. R. Chim.*, 2006, **9**, 750–760.
120 B. Erdem, E. D. Sudol, V. L. Dimonie and M. S. El-Aasser, *J. Polym. Sci., Part A: Polym. Chem.*, 2000, **38**, 4419–4430.
121 B. Erdem, E. D. Sudol, V. L. Dimonie and M. S. El-Aasser, *J. Polym. Sci., Part A: Polym. Chem.*, 2000, **38**, 4431–4440.
122 B. Erdem, E. D. Sudol, V. L. Dimonie and M. S. El-Aasser, *J. Polym. Sci., Part A: Polym. Chem.*, 2000, **38**, 4441–4450.
123 X. Li, M. Lu, S. Ai, Y. Xiao, C. Zhu and Z. Ai, *J. Adhes. Sci. Technol.*, 2015, **29**, 2049–2064.
124 X. Song, G. Yin, Y. Zhao, H. Wang and Q. Du, *J. Polym. Sci., Part A: Polym. Chem.*, 2009, **47**, 5728–5736.
125 G. Yin, Z. Zheng, H. Wang and Q. Du, *J. Colloid Interface Sci.*, 2011, **361**, 456–464.
126 Y. Zhao, H. Wang, X. Song and Q. Du, *Macromol. Chem. Phys.*, 2010, **211**, 2517–2529.
127 M. Y. Mamaghani, M. Pishvaei and B. Kaffashi, *Macromol. Res.*, 2011, **19**, 243–249.
128 S. Jairam, Z. Tong, L. Wang and B. Welt, *ACS Sustainable Chem. Eng.*, 2013, **1**, 1630–1637.
129 S. A. Kedzior, H. S. Marway and E. D. Cranston, *Macromolecules*, 2017, **50**, 2645–2655.
130 L. Liu, Z. Hu, X. Sui, J. Guo, E. D. Cranston and Z. Mao, *Ind. Eng. Chem. Res.*, 2018, **57**, 7169–7180.
131 L. Bai, L. G. Greca, W. Xiang, J. Lehtonen, S. Huan, R. W. N. Nugroho, B. L. Tardy and O. J. Rojas, *Langmuir*, 2019, **35**(3), 571–588.
132 S. A. Kedzior, M. A. Dubé and E. D. Cranston, *ACS Sustainable Chem. Eng.*, 2017, **5**, 10509–10517.

133 V. Brunella, S. A. Jadhav, I. Miletto, G. Berlier, E. Ugazio, S. Sapino and D. Scalarone, *React. Funct. Polym.*, 2016, **98**, 31–37.
134 B. Peng and Y. Chen, *Macromol. Rapid Commun.*, 2013, **34**, 1169–1173.
135 J. J. Chung, J. R. Jones and T. K. Georgiou, *Macromol. Rapid Commun.*, 2015, **36**, 1806–1809.
136 J. J. Chung, S. Li, M. M. Stevens, T. K. Georgiou and J. R. Jones, *Chem. Mater.*, 2016, **28**, 6127–6135.
137 S. W. Zhang, S. X. Zhou, Y. M. Weng and L. M. Wu, *Langmuir*, 2006, **22**, 4674–4679.
138 K. F. Ni, G. R. Shan and Z. X. Weng, *Macromolecules*, 2006, **39**, 2529–2535.
139 Z. H. Cao, G. R. Shan, G. Fevotte, N. S. Othman and E. Bourgeat-Lami, *Macromolecules*, 2008, **41**, 5166–5173.
140 Y. Luo, H. Xu and B. Zhu, *Polymer*, 2006, **47**, 4959–4966.
141 S. Yang, C. Song, T. Qiu, L. Guo and X. Li, *Langmuir*, 2013, **29**, 92–101.
142 I. Tissot, C. Novat, F. Lefebvre and E. Bourgeat-Lami, *Macromolecules*, 2001, **34**, 5737–5739.
143 C. N. I. Tissot, F. Lefebvre and E. B. Lami, *Macromolecules*, 2001, **34**, 5737–5739.
144 I. Tissot, J. P. Reymond, F. Lefebvre and E. Bourgeat-Lami, *Chem. Mater.*, 2002, **14**, 1325–1331.
145 B. Yang, J. Zhang, J. Lin, B. Wu, Q. Liu, W. Yang, M. Wu, Q. Wu and J. Yang, *Macromol. Res.*, 2013, **21**, 123–126.
146 X. Zhang, Y. Sun, Y. Mao, K. Chen, Z. Cao and D. Qi, *RSC Adv.*, 2018, **8**, 3910–3918.
147 J. Zhang, M. Wu, Q. Wu, J. Yang, N. Liu and Z. Jin, *Chem. Lett.*, 2010, **39**, 206–207.
148 X. Han, S. Huang, Y. Wang and D. Shi, *Mater. Sci. Eng., C*, 2016, **64**, 87–92.
149 Y. Wu, Y. Zhang, J. Xu, M. Chen and L. Wu, *J. Colloid Interface Sci.*, 2010, **343**, 18–24.
150 R. G. Gilbert, *Emulsion Polymerisation: A Mechanistic Approach*, Academic Press, San Diego, 1995.
151 S. C. Thickett and R. G. Gilbert, *Polymer*, 2007, **48**, 6965–6991.
152 W. D. Hergeth, W. Lebek, R. Kakuschke and K. Schmutzler, *Makromol. Chem.*, 1991, **192**, 2265–2275.
153 W. D. Hergeth, W. Lebek, E. Stettin, K. Witkowski and K. Schmutzler, *Makromol. Chem.*, 1992, **193**, 1607–1621.
154 F. K. Hansen and J. Ugelstad, *J. Polym. Sci., Part A: Polym. Chem.*, 1979, **17**, 3033–3045.
155 E. Giannetti, *AIChE J.*, 1993, **39**, 1210–1227.
156 S. U. Pickering, *J. Chem. Soc., Trans.*, 1907, **91**, 2001–2021.
157 W. Ramsden and F. Gotch, *Proc. R. Soc. London*, 1904, **72**, 156–164.
158 A. Schrade, K. Landfester and U. Ziener, *Chem. Soc. Rev.*, 2013, **42**, 6823–6839.
159 M. Nomura, H. Tobita and K. Suzuki, in *Polymer Particles: -/-*, ed. M. Okubo, Springer Berlin Heidelberg, Berlin, Heidelberg, 2005, pp. 1–128, DOI: 10.1007/b100116.
160 N. Sheibat-Othman, H. M. Vale, J. M. Pohn and T. F. L. McKenna, *Macromol. React. Eng.*, 2017, **11**, 1600059.
161 J. Herrera-Ordonez, R. Olayo and S. Carro, *J. Macromol. Sci., Polym. Rev.*, 2004, **C44**, 207–229.
162 P. Daswani and A. van Herk, *Macromol. Theory Simul.*, 2011, **20**, 614–620.
163 P. J. Colver, C. A. L. Colard and S. A. F. Bon, *J. Am. Chem. Soc.*, 2008, **130**, 16850–16851.
164 M. J. Percy, J. I. Amalvy, D. P. Randall, S. P. Armes, S. J. Greaves and J. F. Watts, *Langmuir*, 2004, **20**, 2184–2190.
165 M. J. Percy, V. Michailidou, S. P. Armes, C. Perruchot, J. F. Watts and S. J. Greaves, *Langmuir*, 2003, **19**, 2072–2079.
166 M. Chen, L. Wu, S. Zhou and B. You, *Macromolecules*, 2004, **37**, 9613–9619.
167 T. Rodrigues Guimarães, T. de Camargo Chaparro, F. D'Agosto, M. Lansalot, A. Martins Dos Santos and E. Bourgeat-Lami, *Polym. Chem.*, 2014, **5**, 6611–6622.
168 R. F. A. Teixeira, H. S. McKenzie, A. A. Boyd and S. A. F. Bon, *Macromolecules*, 2011, **44**, 7415–7422.
169 B. Brunier, N. Sheibat-Othman, Y. Chevalier and É. Bourgeat-Lami, *AIChE J.*, 2018, **64**, 2612–2624.
170 A. Lotierzo and S. A. F. Bon, *Polym. Chem.*, 2017, **8**, 5100–5111.
171 H. Wang, V. Singh and S. H. Behrens, *J. Phys. Chem. Lett.*, 2012, **3**, 2986–2990.
172 B. zu Putlitz, K. Landfester, H. Fischer and M. Antonietti, *Adv. Mater.*, 2001, **13**, 500–503.
173 D. Nguyen, H. S. Zondanos, J. M. Farrugia, A. K. Serelis, C. H. Such and B. S. Hawkett, *Langmuir*, 2008, **24**, 2140–2150.
174 S. I. Ali, J. P. A. Heuts, B. S. Hawkett and A. M. van Herk, *Langmuir*, 2009, **25**, 10523–10533.
175 P. Das and J. P. Claverie, *J. Polym. Sci., Part A: Polym. Chem.*, 2012, **50**, 2802–2808.
176 W. Zhong, J. N. Zeuna and J. P. Claverie, *J. Polym. Sci., Part A: Polym. Chem.*, 2012, **50**, 4403–4407.
177 D. Nguyen, C. H. Such and B. S. Hawkett, *J. Polym. Sci., Part A: Polym. Chem.*, 2013, **51**, 250–257.
178 M. A. Mballa Mballa, S. I. Ali, J. P. A. Heuts and A. M. van Herk, *Polym. Int.*, 2012, **61**, 861–865.
179 D. Nguyen, C. Such and B. Hawkett, *J. Polym. Sci., Part A: Polym. Chem.*, 2012, **50**, 346–352.
180 V. T. Huynh, D. Nguyen, C. H. Such and B. S. Hawkett, *J. Polym. Sci., Part A: Polym. Chem.*, 2015, **53**, 1413–1421.
181 J.-C. Daigle and J. P. Claverie, *J. Nanomater.*, 2008, **2008**, 609184.
182 X. G. Qiao, O. Lambert, J. C. Taveau, P. Y. Dugas, B. Charleux, M. Lansalot and E. Bourgeat-Lami, *Macromolecules*, 2017, **50**, 3796–3806.
183 X. G. Qiao, P. Y. Dugas, B. Charleux, M. Lansalot and E. Bourgeat-Lami, *Polym. Chem.*, 2017, **8**, 4014–4029.
184 O. P. Loiko, A. B. Spoelstra, A. M. van Herk, J. Meuldijk and J. P. A. Heuts, *Polym. Chem.*, 2016, **7**, 3383–3391.
185 O. P. Loiko, A. B. Spoelstra, A. M. van Herk, J. Meuldijk and J. P. A. Heuts, *RSC Adv.*, 2016, **6**, 80748–80755.

186 O. P. Loiko, A. B. Spoelstra, A. M. van Herk, J. Meuldijk and J. P. A. Heuts, *Polym. Chem.*, 2017, **8**, 2909–2912.
187 O. P. Loiko, A. B. Spoelstra, A. M. van Herk, J. Meuldijk and J. P. A. Heuts, *Macromol. React. Eng.*, 2018, **12**, 1700051.
188 E. Bourgeat-Lami, A. J. P. G. França, T. C. Chaparro, R. D. Silva, P. Y. Dugas, G. M. Alves and A. M. Santos, *Macromolecules*, 2016, **49**, 4431–4440.
189 F. Dalmas, S. Pearson, B. Gary, J.-M. Chenal, E. Bourgeat-Lami, V. Prévot and L. Chazeau, *Polym. Chem.*, 2018, **9**, 2590–2600.
190 A. C. Perreira, S. Pearson, D. Kostadinova, F. Leroux, F. D'Agosto, M. Lansalot, E. Bourgeat-Lami and V. Prevot, *Polym. Chem.*, 2017, **8**, 1233–1243.
191 N. Zgheib, J.-L. Putaux, A. Thill, E. Bourgeat-Lami, F. D'Agosto and M. Lansalot, *Polym. Chem.*, 2013, **4**, 607–614.
192 J. Garnier, J. Warnant, P. Lacroix-Desmazes, P.-E. Dufils, J. Vinas, Y. Vanderveken and A. M. van Herk, *Macromol. Rapid Commun.*, 2012, **33**, 1388–1392.
193 W.-M. Wan, C.-Y. Hong and C.-Y. Pan, *Chem. Commun.*, 2009, 5883–5885, DOI: 10.1039/B912804B.
194 J.-T. Sun, C.-Y. Hong and C.-Y. Pan, *Polym. Chem.*, 2013, **4**, 873–881.
195 J. Rieger, *Macromol. Rapid Commun.*, 2015, **36**, 1458–1471.
196 S. L. Canning, G. N. Smith and S. P. Armes, *Macromolecules*, 2016, **49**, 1985–2001.
197 B. Charleux, G. Delaittre, J. Rieger and F. D'Agosto, *Macromolecules*, 2012, **45**, 6753–6765.
198 J. N. Israelachvili, *Intermolecular and Surface Forces*, Academic, London, 2nd edn, 1992.
199 D. M. Vriezema, M. Comellas Aragonès, J. A. A. W. Elemans, J. J. L. M. Cornelissen, A. E. Rowan and R. J. M. Nolte, *Chem. Rev.*, 2005, **105**, 1445–1490.
200 M. Semsarilar, V. Ladmiral, A. Blanazs and S. P. Armes, *Langmuir*, 2011, **28**, 914–922.
201 M. Semsarilar, V. Ladmiral, A. Blanazs and S. P. Armes, *Langmuir*, 2012, **29**, 7416–7424.
202 P. Yang, L. P. D. Ratcliffe and S. P. Armes, *Macromolecules*, 2013, **46**, 8545–8556.
203 X. Zhang, S. Boisse, C. Bui, P.-A. Albouy, A. Brulet, M.-H. Li, J. Rieger and B. Charleux, *Soft Matter*, 2012, **8**, 1130–1141.
204 N. J. Warren, O. O. Mykhaylyk, D. Mahmood, A. J. Ryan and S. P. Armes, *J. Am. Chem. Soc.*, 2013, **136**, 1023–1033.
205 S. Sugihara, A. Blanazs, S. P. Armes, A. J. Ryan and A. L. Lewis, *J. Am. Chem. Soc.*, 2011, **133**, 15707–15713.
206 L. A. Fielding, J. A. Lane, M. J. Derry, O. O. Mykhaylyk and S. P. Armes, *J. Am. Chem. Soc.*, 2014, **136**, 5790–5798.
207 L. A. Fielding, M. J. Derry, V. Ladmiral, J. Rosselgong, A. M. Rodrigues, L. P. D. Ratcliffe, S. Sugihara and S. P. Armes, *Chem. Sci.*, 2013, **4**, 2081–2087.
208 X. Zhang, J. Rieger and B. Charleux, *Polym. Chem.*, 2012, **3**, 1502–1509.
209 A. B. Lowe, *Polymer*, 2016, **106**, 161–181.
210 Y. Deng, C. Yang, C. Yuan, Y. Xu, J. Bernard, L. Dai and J. F. Gérard, *J. Polym. Sci., Part A: Polym. Chem.*, 2013, **51**, 4558–4564.
211 B. Karagoz, J. Yeow, L. Esser, S. M. Prakash, R. P. Kuchel, T. P. Davis and C. Boyer, *Langmuir*, 2014, **30**, 10493–10502.
212 R. Bleach, B. Karagoz, S. M. Prakash, T. P. Davis and C. Boyer, *ACS Macro Lett.*, 2014, **3**, 591–596.
213 G. H. Teo, R. P. Kuchel, P. B. Zetterlund and S. C. Thickett, *Polym. Chem.*, 2016, **7**, 6575–6585.
214 W. M. Wan, C. Y. Hong and C. Y. Pan, *Chem. Commun.*, 2009, 5883–5885.
215 W.-M. Wan and C.-Y. Pan, *Polym. Chem.*, 2010, **1**, 1475–1484.
216 V. P. Torchilin, *Nat. Rev. Drug Discovery*, 2005, **4**, 145.
217 M. Antonietti and S. Förster, *Adv. Mater.*, 2003, **15**, 1323–1333.
218 R. P. Brinkhuis, F. P. J. T. Rutjes and J. C. M. van Hest, *Polym. Chem.*, 2011, **2**, 1449–1462.
219 C. Sanson, C. Schatz, J.-F. Le Meins, A. Soum, J. Thévenot, E. Garanger and S. Lecommandoux, *J. Controlled Release*, 2010, **147**, 428–435.
220 R. Deng, M. J. Derry, C. J. Mable, Y. Ning and S. P. Armes, *J. Am. Chem. Soc.*, 2017, **139**, 7616–7623.
221 C. J. Mable, M. J. Derry, K. L. Thompson, L. A. Fielding, O. O. Mykhaylyk and S. P. Armes, *Macromolecules*, 2017, **50**, 4465–4473.
222 C. J. Mable, R. R. Gibson, S. Prevost, B. E. McKenzie, O. O. Mykhaylyk and S. P. Armes, *J. Am. Chem. Soc.*, 2015, **137**, 16098–16108.
223 D. Zhang, K. L. Thompson, R. Pelton and S. P. Armes, *Langmuir*, 2010, **26**, 17237–17241.
224 N. J. W. Penfold, J. R. Lovett, P. Verstraete, J. Smets and S. P. Armes, *Polym. Chem.*, 2017, **8**, 272–282.
225 J. R. Lovett, N. J. Warren, S. P. Armes, M. J. Smallridge and R. B. Cracknell, *Macromolecules*, 2016, **49**, 1016–1025.
226 J. Tan, D. Liu, X. Zhang, C. Huang, J. He, Q. Xu, X. Li and L. Zhang, *RSC Adv.*, 2017, **7**, 23114–23121.
227 J. Tan, H. Sun, M. Yu, B. S. Sumerlin and L. Zhang, *ACS Macro Lett.*, 2015, **4**, 1249–1253.
228 Y. Zheng, Y. Huang, Z. M. Abbas and B. C. Benicewicz, *Polym. Chem.*, 2016, **7**, 5347–5350.
229 Y. Zheng, Y. Huang, Z. M. Abbas and B. C. Benicewicz, *Polym. Chem.*, 2017, **8**, 370–374.

